CHAPTER 9.0

INTERPRETATION OF SOIL PROPERTIES

9.1 INTRODUCTION

The results of the field and laboratory testing program must be compiled into a simplified representation of the subsurface conditions that includes the geostratigraphy and interpreted engineering parameters. Natural geomaterials are particularly difficult to quantify because they exhibit complex behavior and involve the actions and interactions of literally infinite numbers of particles that comprise the soil and/or rock mass. In contrast to the more "well-behaved" civil engineering materials, soils are affected by their initial stress state, direction of loading, composition, drainage conditions, and loading rate.

Whereas the properties of man-made materials (e.g., brick, concrete, steel) can be varied on demand, soil and rock formations have already been provided by Mother Nature, and in many cases, have been situated in-place for many thousands of years. Thus, the properties of soil and rock properties must be evaluated through a program of limited testing and sampling. In certain cases, the soil properties may be altered or changed using ground modification techniques. Moreover, in many situations, the ground conditions must be left as is because of the impracticality of addressing such large masses of material within economic and timely considerations. Therefore, a geotechnical site characterization of the geomaterials must be made using a selection of geophysics, drilling, sampling, in-situ testing, and laboratory methods.

All interpretations of geotechnical data will involve a degree of uncertainty because of the differing origins, inherent variability, and innumerable complexities associated with natural materials. The interpretations of soil parameters and properties will rely on a combination of direct assessment by laboratory testing of recovered undisturbed samples and in-situ field data that are evaluated by theoretical, analytical, statistical, and empirical relationships. Usually, there are far fewer laboratory tests than field tests because of the greater time and expense involved in conducting the lab tests. It is also more difficult to acquire a reliable set of representative and undisturbed samples of the various soil strata. Therefore, much reliance falls on the more abundant data from in-situ and field tests for evaluating and interpreting soil parameters. The application of empirical correlations and theoretical relationships should be done carefully, with due calibration and verification with the companion sets of laboratory tests, to ensure that proper site characterization is achieved. Notably, many interrelationships between engineering properties and field tests have developed separately from individual sources, with different underlying assumptions, reference basis, and specific intended backgrounds, often for a specific soil.

Emphasis in this chapter is on the interpretation of soil properties from in-situ tests for the analysis and design of foundations, embankments, slopes, and earth-retaining structures in soils. Correlation of properties to laboratory index tests and typical ranges of values are also provided to check the reasonableness of field and laboratory test results. Reference is made to the FHWA Geotechnical Engineering Circular No. 5: *Evaluation of Soil & Rock Properties* (2001) for more detailed directions on the procedures and methodologies, as well as examples of data processing and evaluation. Herein, selected procedures are presented for evaluating geostratigraphy, density, strength, stiffness, and flow characteristics. Generally, these are not unique and singular relationships because of the wide diversity of soil materials worldwide, yet intended to provide a guide to the selection of geotechnical engineering parameters that are needed in stability and deformation analyses.

9.2 COMPOSITION AND CLASSIFICATION

Soil composition includes the relative size distributions of the grain particles, their constituent characteristics (mineralogy, angularity, shape), and porosity (density and void ratio). These can be readily determined by the traditional approach to soil investigation using a drilling & sampling program followed by laboratory testing. Of recent, these methods are complemented by direct-push technologies that infer soil behavioral classifications, including the CPT, DMT, and others. Although no samples are obtained with these latter tests, the directly-measured readings indicate how a particular soil may react to loading, strain rate, and/or flow conditions, therefore aiding in the selection of appropriate engineering parameters. The behavior of soil materials is controlled not only by their constituents, but also by less tangible and less-quantifiable factors as age, cementation, fabric (packing arrangements, inherent structure), stress-state anisotropy, and sensitivity. In-situ tests provide an opportunity to observe the soil materials with all their relevant characteristics under controlled loading conditions.

9.2.1. Soil Classification and Geostratigraphy

In the field, there are three approaches to soil classification and the delineation of geostratigraphy: drilling & sampling, cone penetration, and flat plate dilatometer soundings. Samples taken from the ground often undergo disturbance effects and are therefore well-suited to USCS classification techniques that require total destruction. Testing by the cone and dilatometer measure the in-situ response of soil while in its original position and environment, thus indicating a "soil behavioral" type of classification at the moment of testing. The field tests are primarily conducted by deployment of vertical soundings to determine the type, thickness, and variability of soil layers, depth of bedrock, level of groundwater, and presence of lenses, seams, inclusions, and/or voids. Traditionally, site investigations have been accomplished using rotary drilling and drive sampling methods, as depicted in Figure 9-1. Yet recently, the cone penetrometer and dilatometer have become recognized as expedient and economical exploratory tools in soil deposits. Moreover, these methods should be taken as complementary to each other, rather than substitutional.

9.2.2 Soil Classification by Soil Sampling and Drilling

Routine sampling involves the recovery of auger cuttings, drive samples, and pushed tubes from rotary-drilled boreholes (ASTM D 4700). The boring may be created using solid flight augers ($z < 10$ m), hollow-stem augers ($z < 30$ m), wash-boring techniques ($z < 90$ m), and wire-line techniques (applicable to 200 m or more). At select depths, split-barrel samples are obtained according to ASTM D 1586 and a visual-manual examination of the recovered samples is sufficient for a general quantification of soil type (ASTM D-2488). These 0.3-m long drive samples are collected only at regular 1.5-m intervals, however, and thus reflect only a portion of the subsurface stratigraphy. Less frequently, thin-walled undisturbed tube samples are obtained per ASTM D 1587. More recently, sampling by a combination of direct-push and percussive forces has become available (e.g., geoprobe sampling; sonic drilling), whereby 25-mm diameter continuously-lined plastic tubes of soil are recovered. Although disturbed, the full stratigraphic profile can be examined for soil types, layers, seams, lenses, color changes, and other details.

For soil types, the percent fines (PF) content is a particularly important demarcation of grain sizes. Materials retained on a U.S. No. 200 sieve correspond to particles greater than 0.075 mm in diameter and termed ***granular*** materials. These include sands and gravels that exhibit, for the most part, mechanical properties due to normal and shearing forces. Soils passing the No. 200 sieve (smaller than 0.075 mm) are called ***fines*** or ***fine-grained*** soils. These include silt-, clay-, and colloidal-size materials that, in addition to responding to normal and shear stresses, can have properties which are significantly affected by micro-level phenomena including chemical reactions, electrical forces, capillary hydraulics, and bonding.

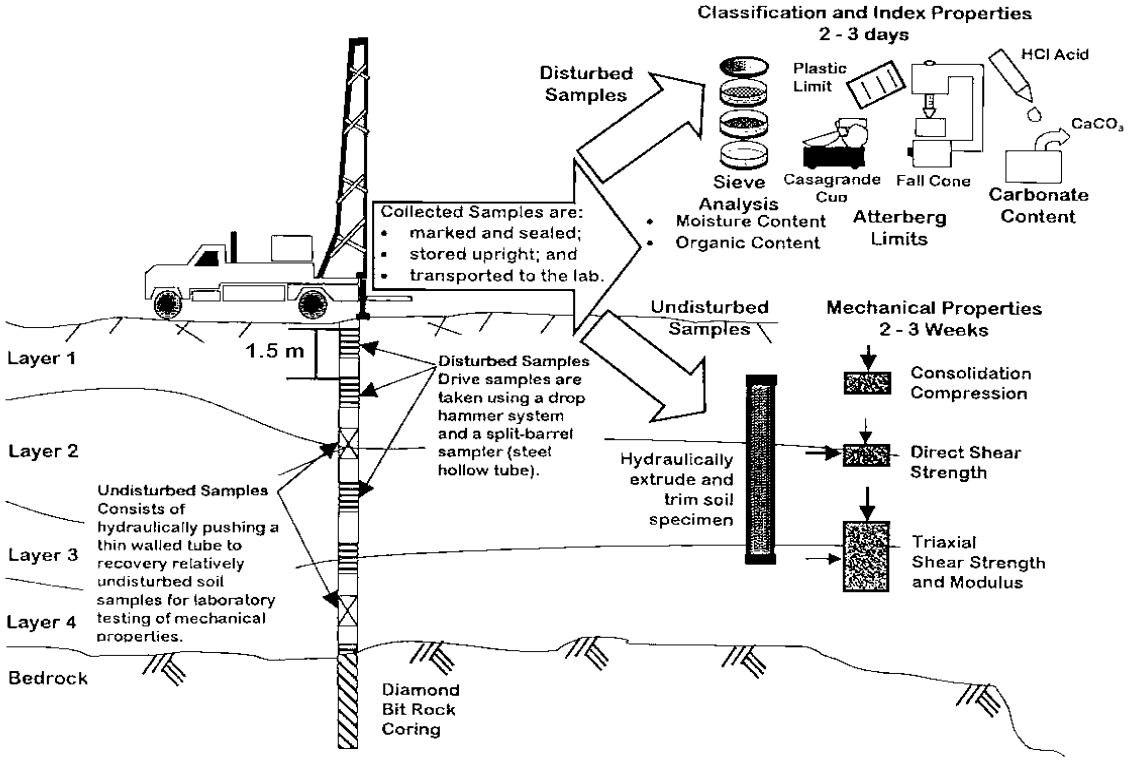

Figure 9-1. Delineation of Geostratigraphy and Soil & Rock Types by Drill & Sampling Methods.

A difficulty with the USCS system is its reliance on disaggregated and remolded samples. Natural soils exist in the ground in specially-sorted arrangements and particle assemblages, in some instances with bonded or cemented particles, complex fabric, varves, seams, layering sequences, sensitivity, and aging effects. The stress-strain-strength-time behavior of soils to loading depends in part upon these special and inherent features. The USCS makes no attempt to quantify any of the unique aspects of this inplace structure, but instead merely relies on a cumulative counting of particle sizes and two remolded indices**.** Consequently, there are a number of instances (e.g., marine deposits, sensitive clays, cemented sands) where the USCS fails to warn the engineer that some unusual behavioral responses or difficulties that may occur during construction in these geomaterials.

Imagine the innumerable possibilities of varied soil types when considering, for example, a clayey sand (SC). The USCS permits this classification for a predominantly sandy material having more than fifty percent of the grain size retained on a No. 200 sieve. The fines may range anywhere from 16 to 49 percent fines and the plasticity tests on material passing a No. 40 sieve fall above the A-line. The composition of the sand particles may either be quartz or feldspar or calcium carbonate or other, or alternatively, a combination of many minerals. The particles of sand may be angular or rounded, or subangular or subrounded. The percentage of fines may consist of silts and/or clays of different mineralogies (e.g., illite, kaolin, montmorillonite, smectite, diatoms, or other). These combinations of coarse- and fine-grained particles may have been placed together in recent times (e.g., Holocene soil < 10,000 years ago) or existed as a more aged soil that weathered into its present makeup many millennia ago (e.g., Cretaceous soil < 120 million years ago). The clayey sand may exist under loose and normally-consolidated conditions as an

intact material, or perhaps became heavily overconsolidated to the point of being fissured, with cracks now pervasive throughout its matrix. Over time, the soil may have been subjected to freeze-thaw, desiccation, drought, flooding, groundwater chemistry, and other factors. Despite these events, use of the USCS would result in the classification of this material as "SC" without further distinction.

9.2.3. Soil Classification by Cone Penetration Testing

The cone penetrometer provides indirect assessments of soil classification type (in the classical sense) by measuring the response during full-displacement. During a cone penetration test (CPT), the continuously-recorded measurements of tip resistance (q_c), sleeve friction (f_s), and porewater pressures (u_b) are affected by the particle sizes, mineralogy, soil fabric, age, stress state, and other factors, as depicted in Figure 9-2 (Hegazy, 1998). In contrast, laboratory methods provide a mechanical analysis by completely disassembling the soil into grouped particle sizes and remolded fines contents. In the CPT (and DMT), the natural soil behavior is reflected, thus perhaps giving a different vantage point, and alternate classification.

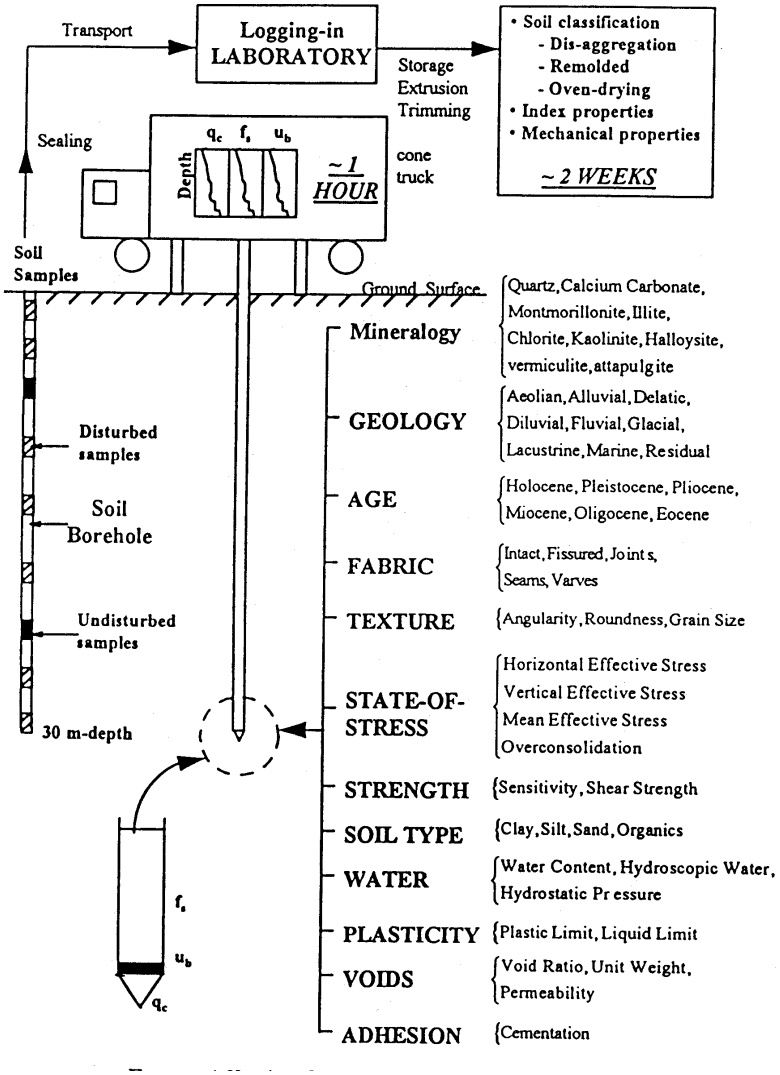

Figure 9-2. Factors Affecting Cone Penetrometer Test Measurements in Soils (Hegazy, 1998).

Soil classification by cone penetrometer involves the use of empirical charts with boundaries between data groupings of similar type. Often, a visual examination of the recorded channel outputs is sufficient to distinguish between fine-grained soils (silts and clays) and coarse-grained materials (sands). Note that the CPT is not used extensively in gravelly soils. In soft to stiff intact clays and silts, it is imperative that the tip resistance be corrected to q_t (Lunne, et al. 1997), as detailed previously in Chapter 5.2. In sands and fissured clays, the correction is often not so significant.

A general *rule of thumb* is that the tip stress in sands is $q_t > 40$ atm (Note: one atmosphere . 1 kg/cm^2 . 1 tsf . 100 kPa), while in many soft to stiff clays and silts, $q_t < 20$ atm. In clean sands, penetration porewater pressures are near hydrostatic values (u_2 . $u_o = (_w z)$ since the permeability is high, while in soft to stiff intact clays, measured u_2 are often 3 to 10 times u_o. Notably, in fissured clays and silts, the shoulder porewater readings can be zero or negative (up to minus one atmosphere, or -100 kPa). With the sleeve friction reading (f_s), a processed value termed the friction ratio (FR) is used:

$$\text{CPT } \textit{Friction Ratio, FR} = R_f = f_s/q_t \tag{9-1}$$

With CPT data, soil classification can be accomplished using a combination of two readings (either q_t and f_s, or q_t and u_b), or with all three readings. For this, it is convenient to define a normalized porewater pressure parameter, B_q, defined by:

$$\textit{Porewater Pressure Parameter, } B_q = \frac{u_2 - u_0}{q_t - \sigma_{vo}} \tag{9-2}$$

A chart using q_t, FR, and B_q is presented in Figure 9-3, indicating twelve classification regions.

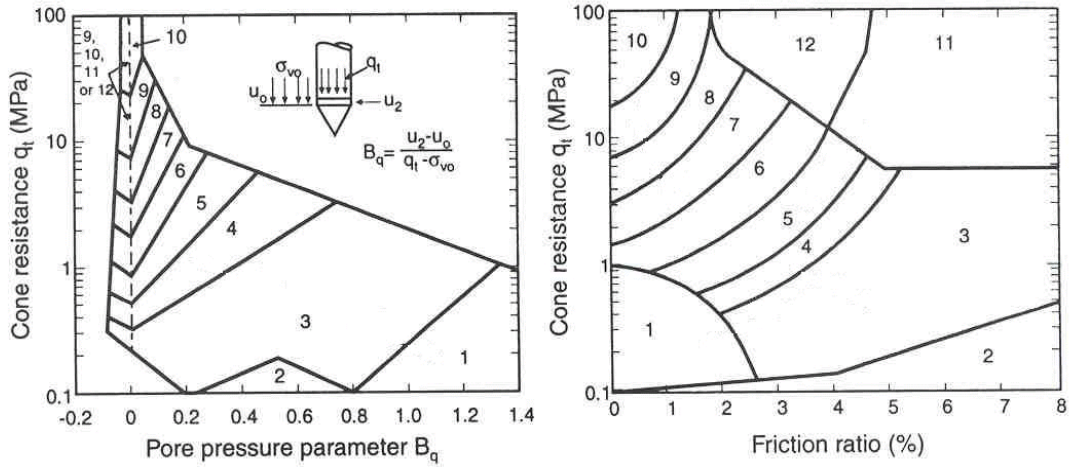

Zone:	Soil Behaviour Type:				
1.	Sensitive fine grained	5.	Clayey silt to silty clay	9.	Sand
2.	Organic material	6.	Sandy silt to clayey silt	10.	Gravelly sand to sand
3.	Clay	7.	Silty sand to sandy silt	11.	Very stiff fine grained*
4.	Silty clay to clay	8.	Sand to silty sand	12.	Sand to clayey sand*

* *Overconsolidated or cemented.*

Figure 9-3. Chart for Soil Behavioral Classification by CPT (Robertson, et al., 1986).

9.2.4 Soil Classification by Flat Dilatometer

Soil classification by flat plate dilatometer tests (DMT) also involves a soil behavioral response. The test can be performed in clay, silt, and sand, but is not appropriate for gravels. A dimensionless material index (I_D) is used to evaluate soil type according to the empirical rules (Marchetti, 1980):

$$\text{DMT Material Index:} \quad I_D = (p_1 - p_o)/(p_o - u_o) \tag{9-3}$$

where p_o = corrected contact pressure and p_1 = corrected expansion pressure, as detailed in Chapter 5.4. For the DMT, the soil types are distinguished by the following ranges: *Clay:* $I_D < 0.6$; *Silt*: $0.6 < I_D < 1.8$; *Sand:* $1.8 > I_D$. Values outside of the range: $0.1 < I_D < 6$ should be checked and verified.

9.3 Density

9.3.1. Unit Weight

The calculations of overburden stresses within a soil mass require evaluations of the unit weight or mass density of the various strata. *Unit weight* is defined as soil weight per unit volume (units of kN/m^3) and denoted by the symbol γ. Soil *mass density* is measured as mass per volume (in either g/cc or kg/m^3) and denoted by ρ. In common use, the terms "unit weight" and "density" are used interchangeably. Their interrelationship is:

$$\gamma = \rho g \tag{9-4}$$

where g = gravitational constant = 9.8 m/sec^2. A reference value for fresh water is adopted, whereby ρ_w = 1 g/cc, and the corresponding γ_w = 9.8 kN/m^3 . In the laboratory, soil unit weight is measured on tube samples of natural soils and depends upon the specific gravity of solids (G_s), water content (w_n), and void ratio (e_0), as well as the degree of saturation (S). These parameters are interrelated by the soil identity:

$$G_s \, w_n = S \, e_0 \tag{9-5}$$

where S = 1 (100%) for saturated soil (generally assumed for soil layers lying below the groundwater table) and S = 0 (assumed for granular soils above the water table). For the case of clays and silts above the water table, the soils may have degrees of saturation between 0 to 100%. Full saturation can occur due to capillarity effects and varies as the atmospheric weather. The identity relationship for total unit weight is:

$$\gamma_T = \frac{(1 + w_n)}{(1 + e_0)} G_s \gamma_w \tag{9-6}$$

When placing compacted fills, field measurements of soil mass density can be made using drive tubes (ASTM D 2937), sand cone method (ASTM D 1556), or nuclear gauge (ASTM D 2922). To obtain unit weights with depth in natural soil formations, either high-quality thin-walled tube samples (ASTM D 1587) or geophysical gamma logging techniques (ASTM D 5195) can be employed. Often, thin-walled tube sampling of clean sands is not viable. Also, sampling at great depths is time consuming and sometimes difficult. Alternatively, the values of γ (and ρ) may be estimated from empirical relationships. For example, since the value of $G_s = 2.7 \pm 0.1$ for many soils, saturated unit weight can be related to the water content by combining (9-5) and (9-6) for S = 1, as illustrated in Figure 9-4. The effects of cementation, geochemical changes, sensitivity, leaching and/or presence of metal oxides or other minerals can result in differences with this trend.

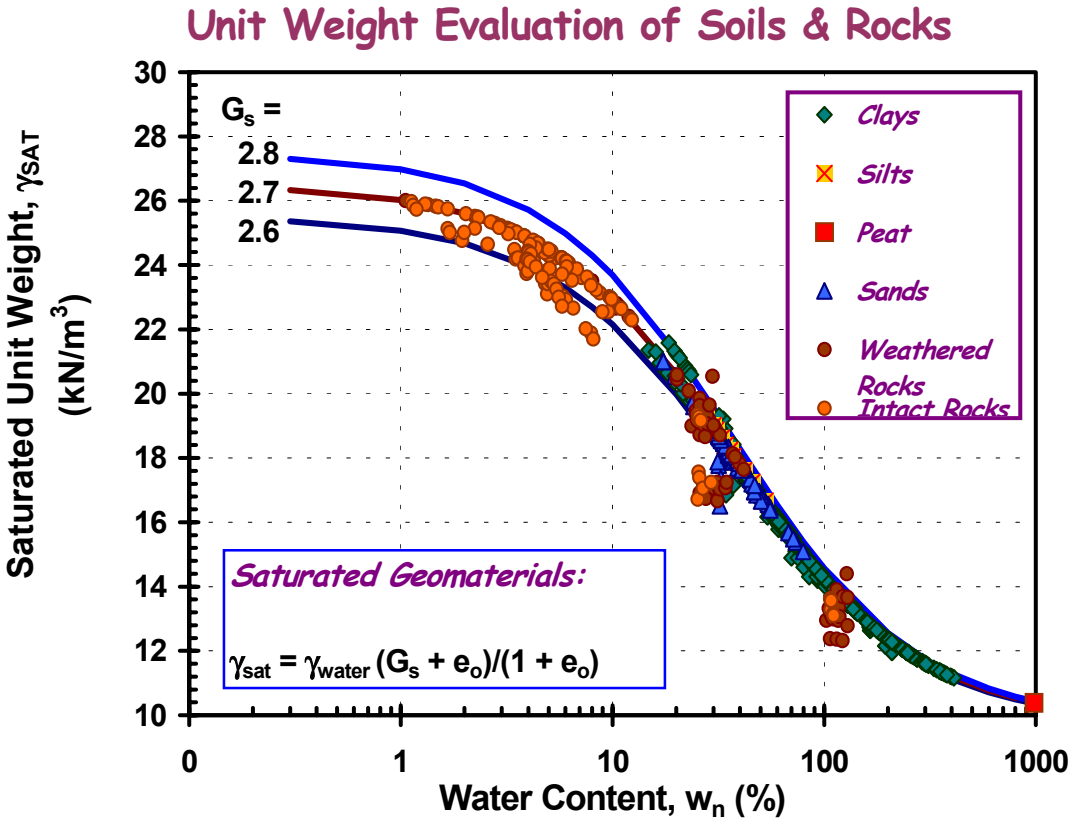

Figure 9-4. Interrelationship Between Saturated Unit Weight and In-Place Water Content of Geomaterials.

During in-situ testing, the in-place water content is not normally measured directly in the field during the site exploration phase. Therefore, if data reduction is sought immediately, a surrogate measure of the in-situ water content (or void ratio) can be made via the results of shear wave velocity (V_s) profiles. Methods for determining V_s in the field are reviewed in Section 5.7. For saturated soils, Figure 9-5 presents an observed relationship between the total unit weight ($(_T)$ in terms of V_s and depth z. Note that for rocks and cemented materials, the trends are distinctly separate from those of particulate geomaterials. The estimation of unit weights for dry to partially saturated soils depends on the degree of saturation, as defined by (9-5) and (9-6).

The total overburden stress (F_{vo}) is calculated from (see Section 7.1.4):

$$F_{vo} = E(_T) z \qquad (9\text{-}7)$$

which in turn is used to obtain the effective vertical overburden stress:

$$F_{vo}r = F_{vo} - u_0 \qquad (9\text{-}8)$$

where the hydrostatic porewater pressure (u_0) is determined from the water table (see equation 7-2).

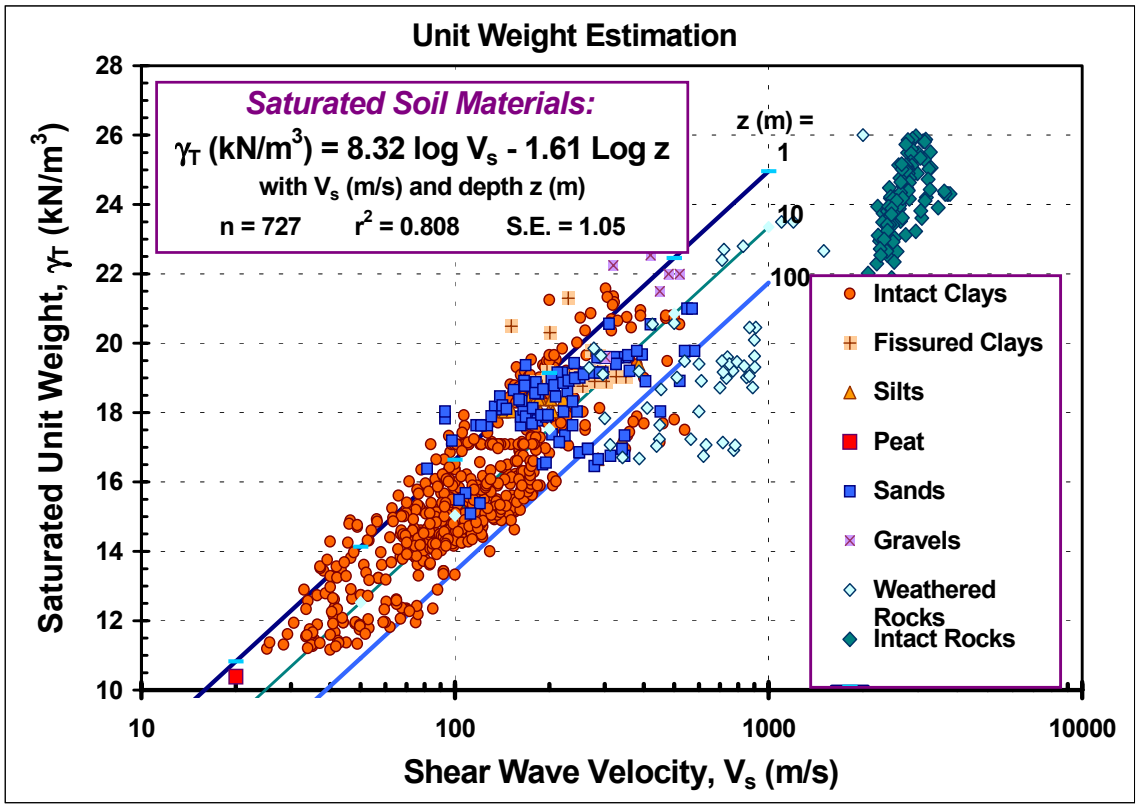

Figure 9-5. Unit Weight Relationship with Shear Wave Velocity and Depth in Saturated Geomaterials. (Note: n = number of data points; r^2 = coefficient of determination; S.E. = standard error of dependent variable).

9.3.2. Relative Density Correlations

The *relative density* (D_R) is used to indicate the degree of packing of sand particles and applicable strictly to granular soils having less than 15 percent fines. The relative density is defined by:

$$D_R = \frac{e_{max} - e_0}{e_{max} - e_{min}} \tag{9-9}$$

where e_{max} = void ratio at the loosest state (ASTM D 4254) and e_{min} = void ratio at the densest state (ASTM D 4253). The direct determination of D_R by the above definition is not common in practice, however, because three separate parameters (e_o, e_{max}, and e_{min}) must be evaluated. Moreover, it is very difficult to directly determine the in-place void ratio of clean sands and granular soils with depth because undisturbed sampling is generally not possible. For a given soil, the maximum and minimum void states are apparently related (Poulos, 1988). A compiled database indicates (n = 304; r^2 = 0.851; S.E. = 0.044):

$$e_{min} = 0.571\, e_{max} \tag{9-10}$$

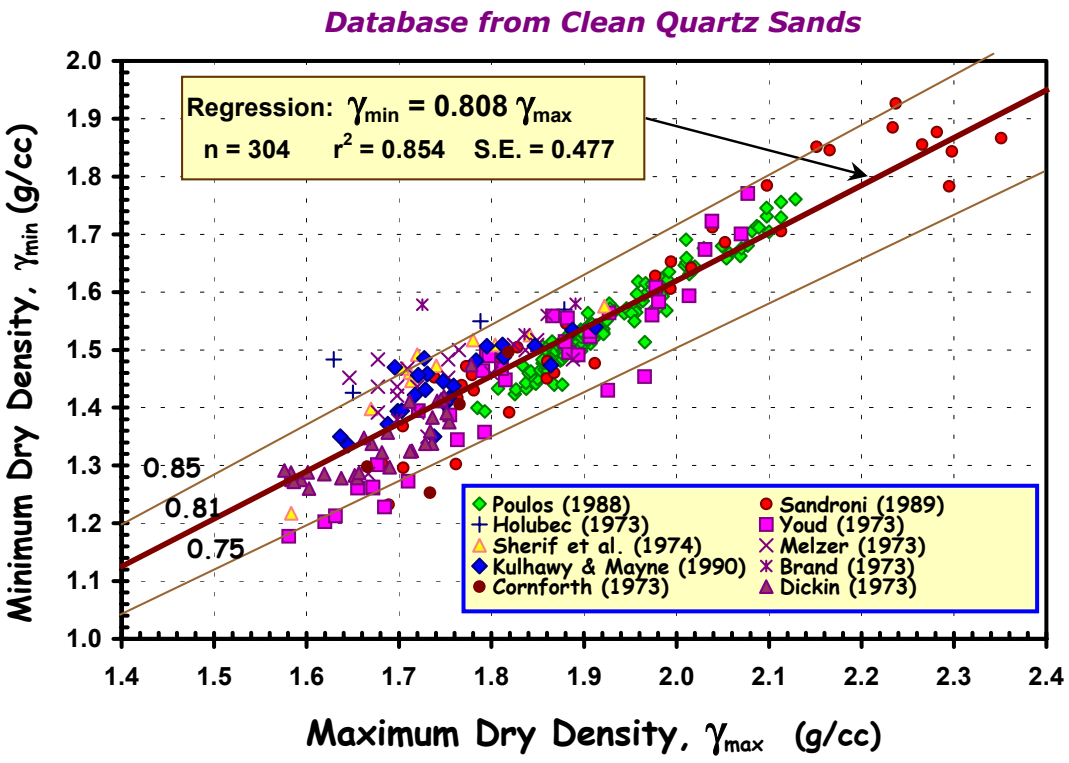

Figure 9-6. Interrelationship Between Minimum and Maximum Dry Densities of Quartz Sands.
(Note: Conversion in terms of mass density and unit weight: 1 g/cc = 9.8 kN/m^3 = 62.4 pcf)

For dry states (w = 0), the dry density is given as: $\gamma_d = G_s \gamma_w/(1+e)$ and the relationship between the minimum and maximum densities is shown in Figure 9-6 for a variety of sands. The mean trend is given by the regression line:

$$\gamma_{d\ (min)} = 0.808\ \gamma_{d\ (max)} \tag{9-11}$$

Laboratory studies by Youd (1973) showed that both e_{max} and e_{min} depend upon uniformity coefficient (UC = D_{60}/D_{10}), as well as particle angularity. For a number of sands (total n = 574), this seems to be borne out by the trend presented in Figure 9-7 for the densest state corresponding to e_{min} and $\gamma_{d\ (max)}$. The correlation for maximum dry density [$\gamma_{d\ (max)}$] in terms of UC for various sands is shown in Figure 9-7 and expressed by (n = 574; r^2 = 0.730):

$$\gamma_{d\ (max)} = 9.8\ [1.65 + 0.52\ \log\ (UC)] \tag{9-12}$$

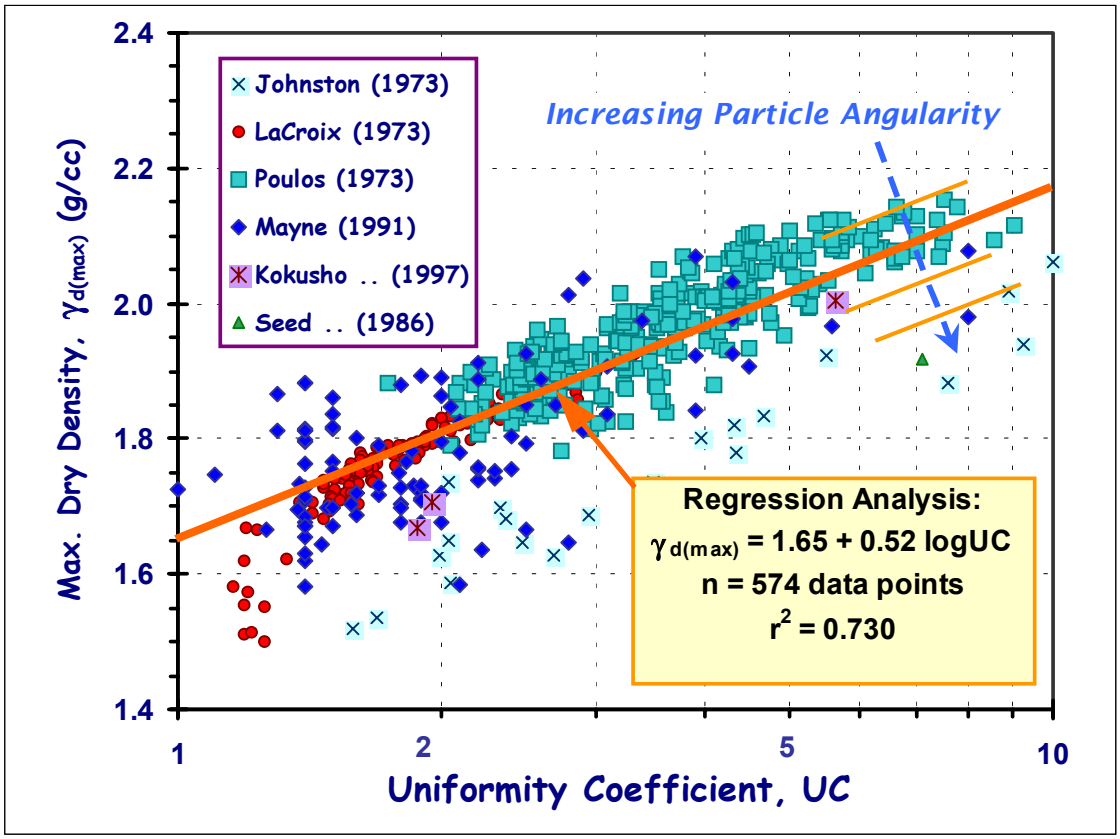

Figure 9-7. Maximum Dry Density Relationship with Sand Uniformity Coefficient (UC = D_{60}/D_{10}).
(Note: Conversion in terms of mass density and unit weight: 1 g/cc = 9.8 kN/m^3 = 62.4 pcf)

From a more practical stance, in-situ penetration test data are used to evaluate the in-place relative density of sands. The original D_R relationship for the SPT suggested by Terzaghi & Peck (1967) has been re-examined by Skempton (1986) and shown reasonable for many quartz sands. The evaluation of relative density (in percent) is given in terms of a normalized resistance [$(N_1)_{60}$], as shown in Figure 9-8:

$$D_R = 100 \cdot \sqrt{\frac{(N_1)_{60}}{60}} \qquad (9\text{-}13)$$

where $(N_1)_{60} = N_{60}/(F_{vo}')^{0.5}$ is the measured N-value corrected to an energy efficiency of 60% and normalized to a stress level of one atmosphere. Note here that the effective overburden stress is given in atmospheres. In a more general fashion, the normalized SPT resistance can be defined by: $(N_1)_{60} = N_{60}/(F_{vo}'/p_a)^{0.5}$ for any units of effective overburden stress, where p_a is a reference stress = 1 bar . 1 kg/cm^2 . 1 tsf . 100 kPa . The range of normalized SPT values should be limited to $(N_1)_{60} < 60$, since above this value, apparent grain crushing occurs due to high dynamic compressive forces. Additional effects of overconsolidation, particle size, and aging may also be considered, as these too affect the correlation (Skempton, 1986; Kulhawy & Mayne, 1990).

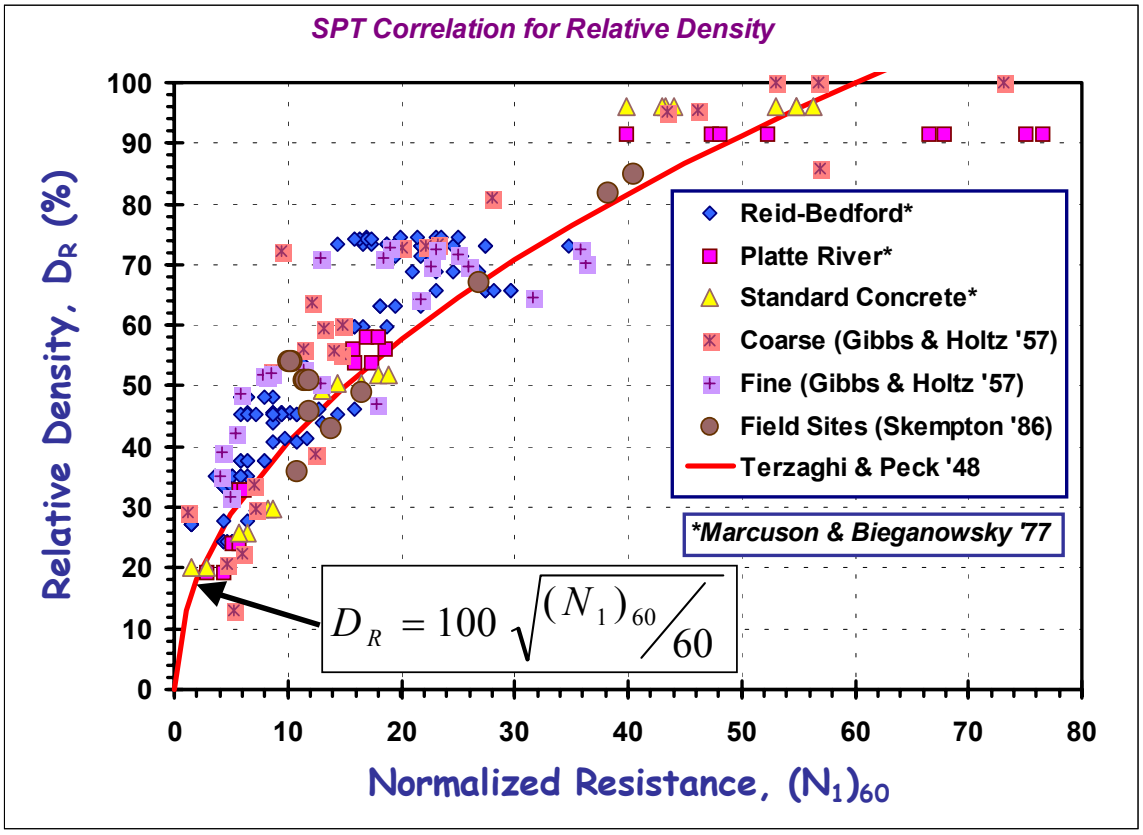

Figure 9-8. Relative Density of Clean Sands from Standard Penetration Test Data.
Note: normalized value $(N_1)_{60} = N_{60}/(F_{vo}r)^{0.5}$ where $F_{vo}r$ is in units of bars or tsf.

A comparable approach for the CPT can be made based on calibration chamber test data on clean quartz sands (Figure 9-9). The trends for relative density (in percent) of unaged uncemented sands are:

Normally-Consolidated Sands: $$D_R = 100\sqrt{\frac{q_{t1}}{300}} \qquad (9\text{-}14a)$$

Overconsolidated Sands: $$D_R = 100\sqrt{\frac{q_{t1}}{300\,OCR^{0.2}}} \qquad (9\text{-}14b)$$

where $q_{t1} = q_c/(F_{vo}')^{0.5}$ is the normalized tip resistance with both the measured q_c and effective overburden stress are in atmospheric units. The relationship should be restricted to $q_{t1} < 300$ because of possible grain crushing effects. For any units of effective overburden stress and cone tip resistance, the normalized value is given by: $q_{t1} = (q_t/p_a)/(F_{vo}'/p_a)^{0.5}$, where p_a is a reference stress = 1 bar . 1 kg/cm^2 . 1 tsf . 100 kPa . Additional effects due to overconsolidation ratio (OCR), mean particle size, soil compressibility, and aging can also be considered (Kulhawy and Mayne, 1991), but these factors are often not well quantified during routine site investigations. As indicated by Figure 9-9b, an increase in OCR in the sand will lower the apparent relative density given by eq (9-13).

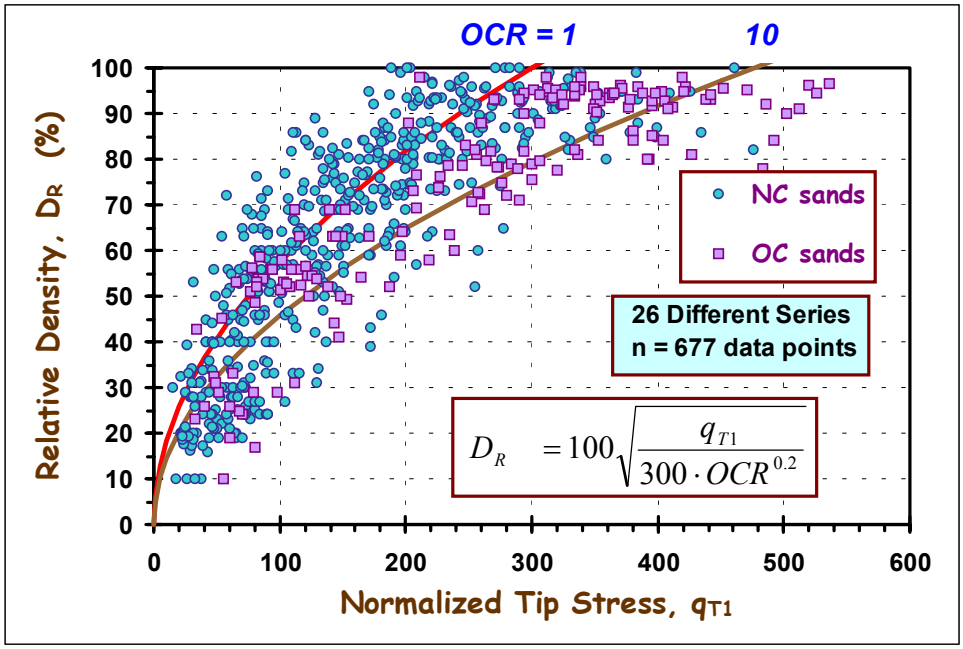

Figure 9-9. Relative Density Evaluations of NC and OC Clean Quartz Sands from CPT Data.
Note: normalized resistance is $q_{t1} = q_c/(F_{vo}')^{0.5}$ with stresses in atmospheres (1 atm . 1 tsf . 100 kPa).

Based on limited flat dilatometer tests (DMT) conducted in the field and calibration chambers, an approximate value of D_R can be obtained from the DMT lateral stress index, as given in Fig. 9-10.

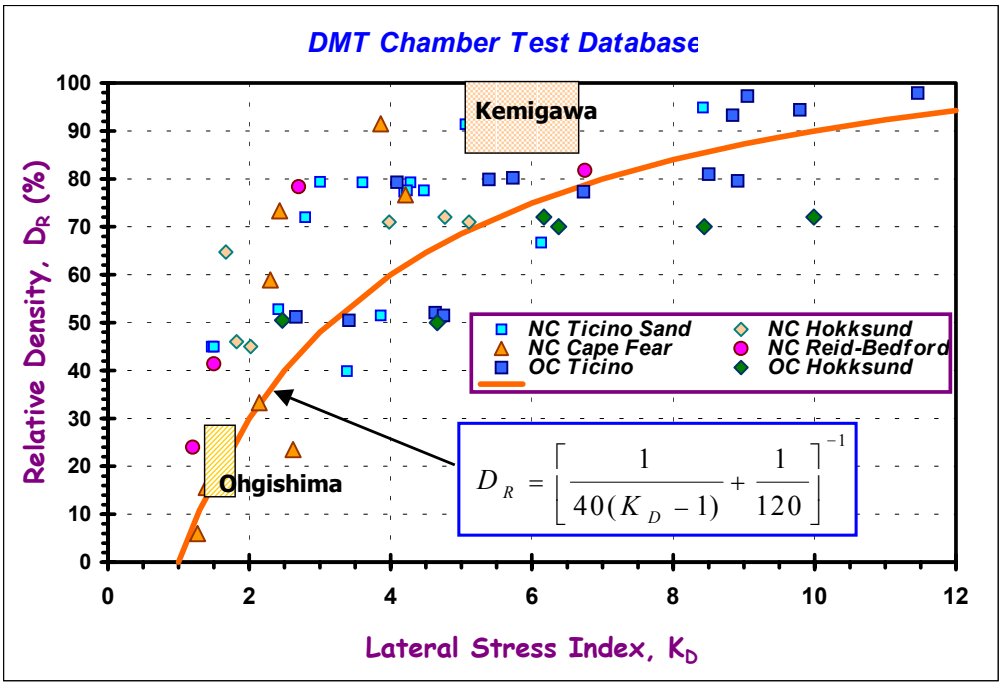

Figure 9-10. Relative Density of Clean Sands Versus DMT Horizontal Stress Index, $K_D = (p_o - u_o)/F_{vo}'$).

9.4. STRENGTH AND STRESS HISTORY

The results of in-situ test measurements are convenient for evaluating the strength of soils and their relative variability across a project site. For sands, the drained strength corresponding to the effective stress friction angle (N_r) is interpreted from the SPT, CPT, DMT, and PMT. For short-term loading of clays and silts, the undrained shear strength (s_u) is appropriate and best determined from normalized relationships with the degree of overconsolidation. In this manner, in-situ test data in clays are used to evaluate the effective preconsolidation stress ($F_p r$) from CPT, CPTu, DMT, and V_s, which in turn provide the corresponding overconsolidation ratios ($OCR = F_p r/F_{vo} r$). The long-term strength of intact clays and silts is represented by the effective stress strength parameters (N_r and $c_r = 0$) that are best determined from either consolidated undrained triaxial tests with porewater pressure measurements, drained triaxial tests, or slow direct shear box tests in the lab. For fissured clay materials, the residual strength parameters ($N_r r$ and $c_r r = 0$) may be appropriate, particularly in slopes and excavations, and these values should be obtained from either laboratory ring shear tests or repeated direct shear box test series.

9.4.1. Drained Friction Angle of Sands

The peak friction angle of sands (N_r) depends on the mineralogy of the particles, level of effective confining stresses, and the packing arrangement (Bolton, 1986). Sands exhibit a nominal value of N_r due solely to mineralogical considerations that corresponds to the critical state (designated $N_{cs} r$). The critical state represents an equilibrium condition for the particles at a given void ratio and effective confining stress level. For clean quartzitic sands, a characteristic $N_{cs} r$. 33°, while a feldspathic sand may show $N_{cs} r$. 30° and a micaceous sandy soil exhibit $N_{cs} r$. 27°. Under many natural conditions, the sands are denser than their loosest states and dilatancy effects contribute to a peak N_r that is is greater than $N_{cs} r$. Figure 9-11 shows typical values of N_r and corresponding unit weights over the full range of cohesionless soils.

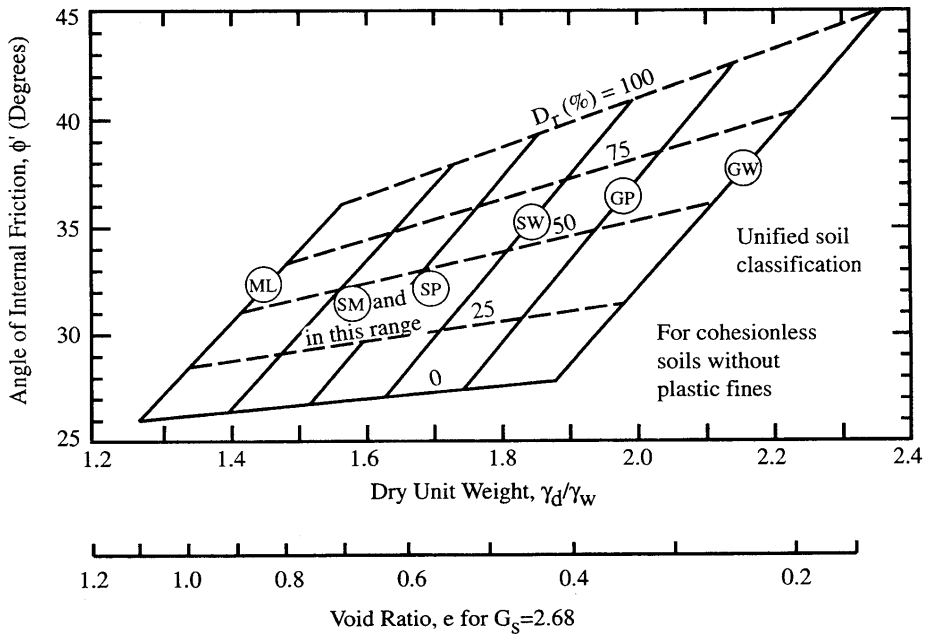

Figure 9-11. Typical Values of N_r and Unit Weight for Cohesionless Soils. (NAVFAC DM 7.1, 1982)

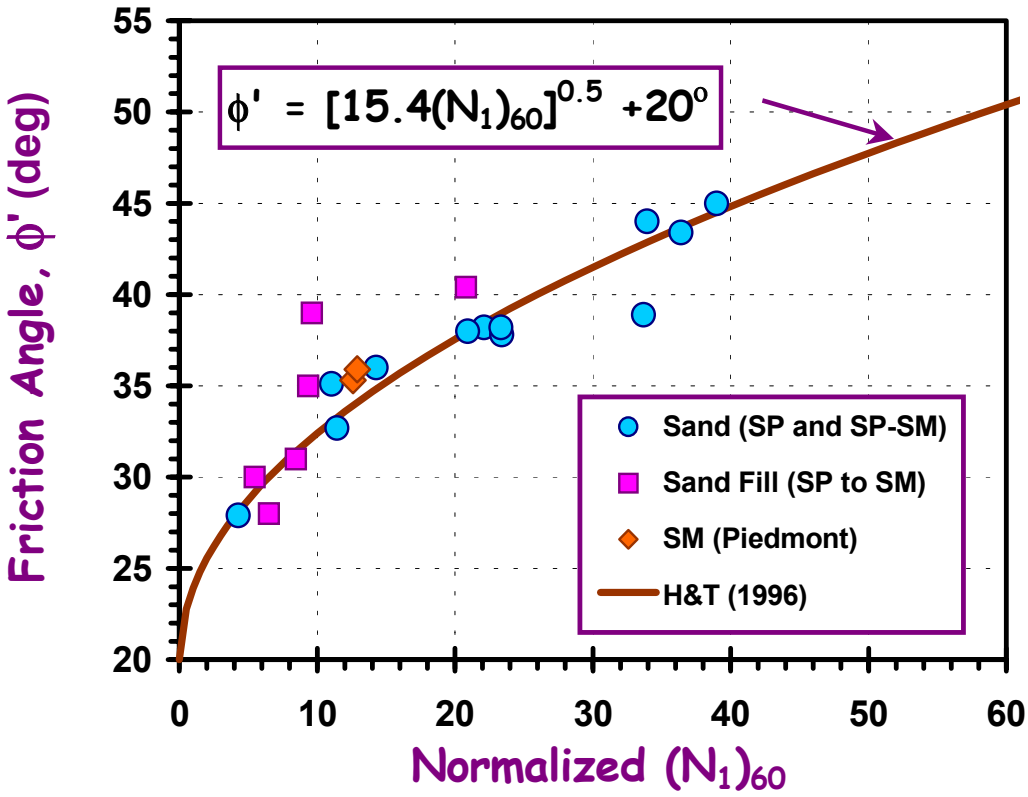

Figure 9-12. Peak Friction Angle of Sands from SPT Resistance (data from Hatanaka & Uchida, 1996). Note: The normalized resistance is $(N_1)_{60} = N_{60}/(F_{vo}'/p_a)^{0.5}$, where p_a = 1 bar . 1 tsf . 100 kPa .

The effective stress friction angle (Nr) of sands is commonly evaluated from in-situ test data. In a recent program, special expensive undisturbed samples of sand were obtained by freezing and, after thawing, tested under triaxial conditions to obtain the peak Nr. These values were subsequently correlated with N-values obtained in the same boreholes and adjacent borings using the energy-corrections and normalization procedures described previously. The peak friction angles (Nr) in terms of the $(N_1)_{60}$ resistances are presented in Figure 9-12.

In one viewpoint, the cone penetrometer can be considered a miniature pile foundation and the measured tip stress (q_T) represented the actual end bearing resistance (q_b). In bearing capacity calculations, the pile end bearing is obtained from limit plasticity theory that indicates: $q_b = N_q F_{vo}r$, where N_q is a bearing capacity factor for surcharge and depends upon the friction angle. Thus, one popular method of interpreting CPT results in sand is to invert the expression ($N_q = q_T / F_{vo}r = fctn$ Nr) to obtain the value of Nr (e.g., Robertson & Campanella, 1983). One method for evaluating the peak Nr of clean quartz sands from normalized CPT tip stresses is presented in Figure 9-13 .

Wedge-plasticity solutions have been developed for determining Nr of clean sands using the flat plate dilatometer test (DMT), as summarized by Marchetti (1997), and these have been recently calibrated with data from different sand types at documented experimental test sites, as shown in Figure 9-14. Theoretical curves are presented for the active (K_A case), at-rest (K_0), and passive earth pressure conditions (K_P case), with the latter giving reasonable values of Nr compared with the experimental data.

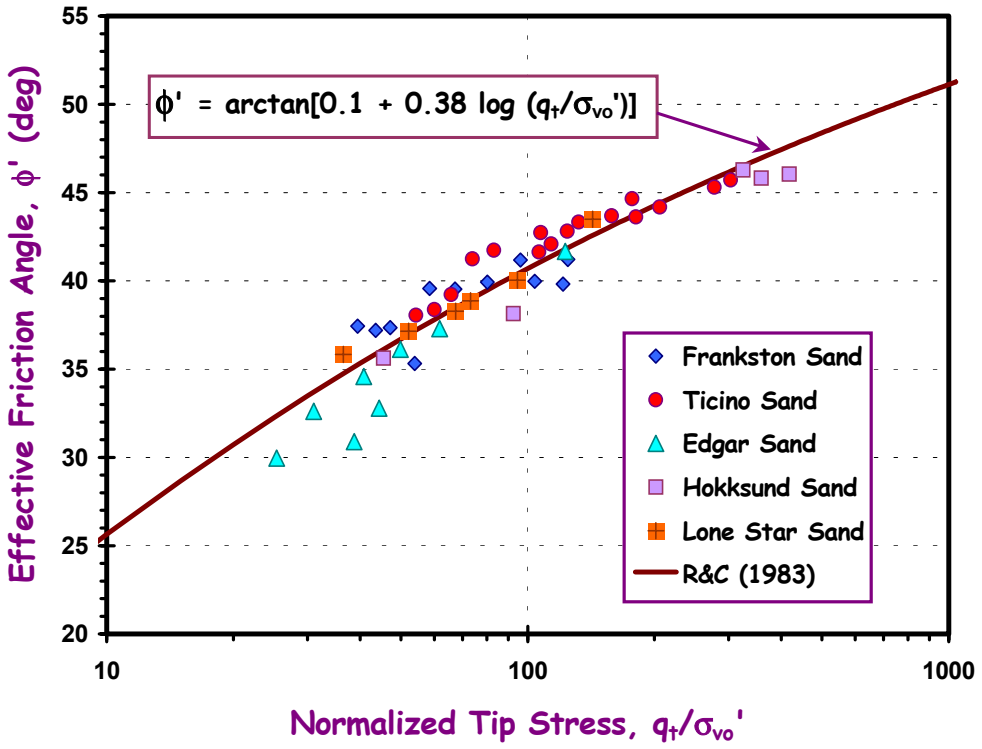

Figure 9-13. Peak Friction Angle of Unaged Clean Quartz Sands from Normalized CPT Tip Resistance. (Calibration Chamber Data Compiled by Robertson & Campanella, 1983).

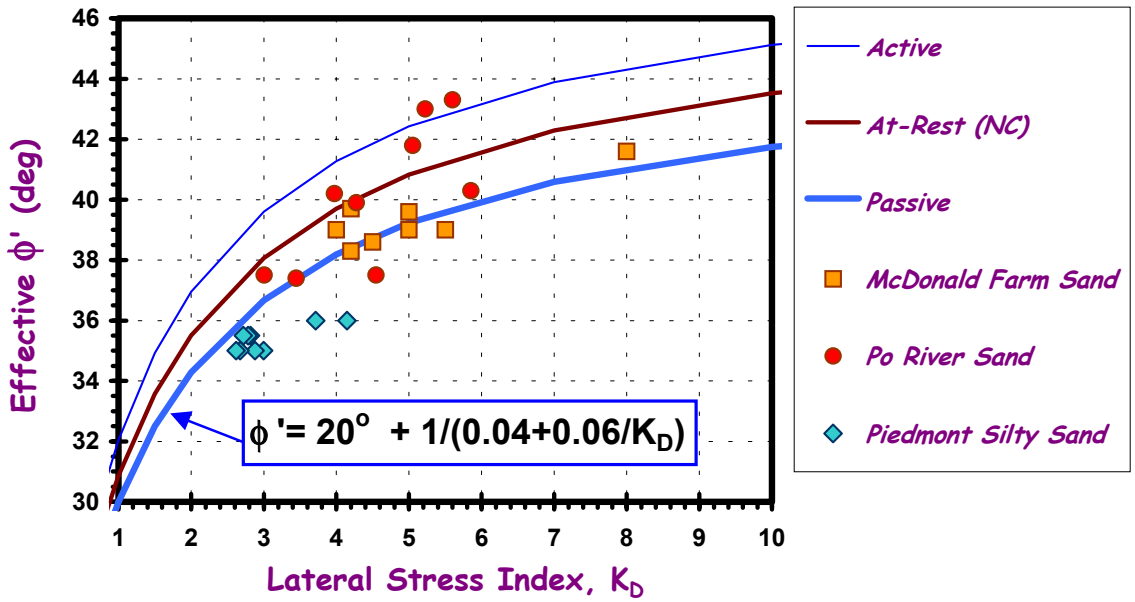

Figure 9-14. Evaluation of Peak Friction Angle of Sands from DMT Results Based on Wedge-Plasticity Solutions (Marchetti, 1997) **and Experimental Data** (Mayne, 2001).

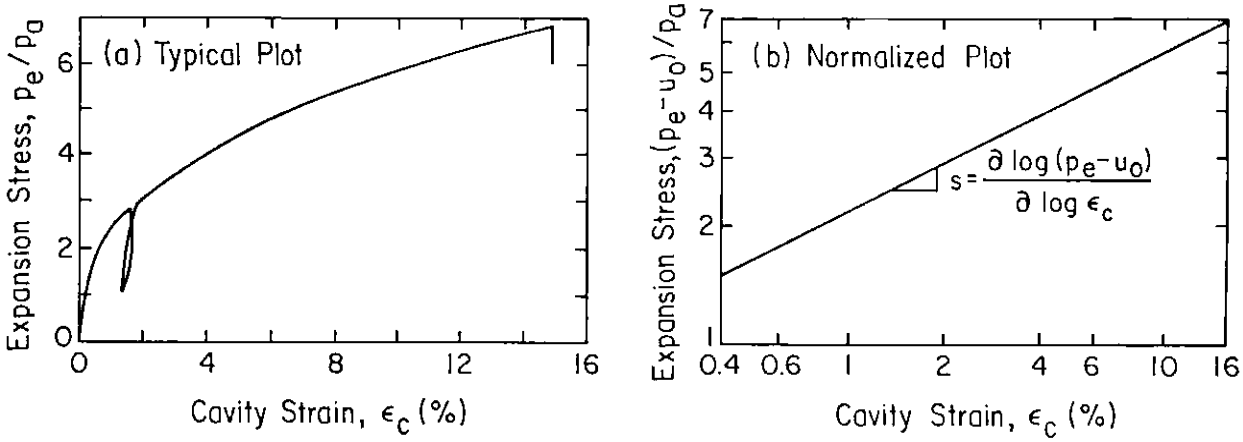

Figure 9-15. Processing of PMT Data in Sands for Peak Nr Determination (after Wroth, 1984).
Note: the term p_a is a reference stress equal to one atmosphere = 1 bar . 100 kPa

The results of pressuremeter tests can be used to evaluate the strength of sands on the basis of dilatancy theory (Wroth, 1984). Figure 9-15 illustrates the processing of the measured expansion pressure curve versus measured cavity strains. Since cavity strain ($\epsilon_c = \Delta r/r_0$) is directly measured during self-boring pressuremeter test (Section 5.5), a conversion to the volumetric strain ($\epsilon_{vol} = \Delta V/V$) obtained during the more common pre-bored pressuremeter is given as:

$$\epsilon_c = (1 - \epsilon_{vol})^{-0.5} - 1 \qquad (9\text{-}15)$$

On a log-log plot of effective pressure ($p_e - u_o$) versus cavity strain (ε_c), the parameter *s* is obtained as the slope (Figure 9-15b), such that $s = \Delta \log (p_e - u_o)/\Delta (\varepsilon_c)$. Together with the corresponding critical state $N_{cv}r$ of the sand (often taken as 33°), the peak Nr for triaxial compression mode is obtained from Fig. 9-16.

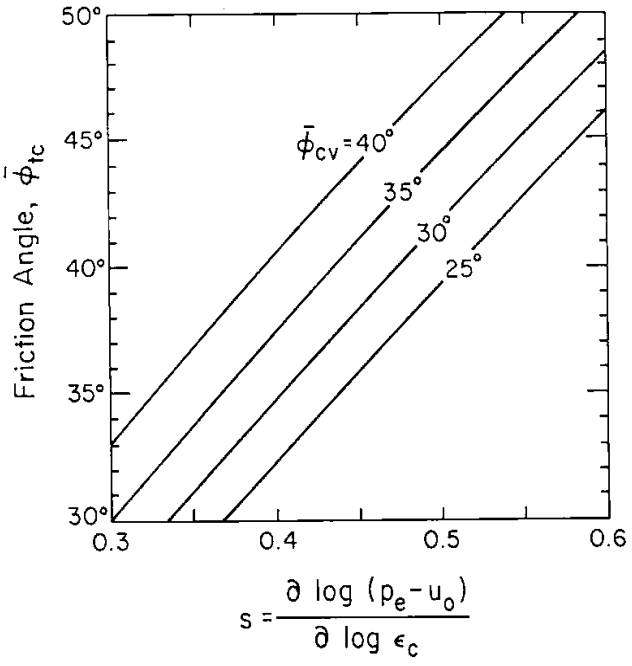

Figure 9-16. Relation Between Peak Nr for Clean Sands and Slope Parameter (*s*) from PMT Data.

9.4.2. Preconsolidation Stress of Clays

The effective preconsolidation stress ($F_p r$) is an important parameter that governs the strength, stiffness, geostatic lateral stress state, and porewater pressure response of soils. It is best determined from one-dimensional oedometer tests (consolidation tests) on high-quality tube samples of the soil. Sampling disturbance, extrusion, and handling effects tend to reduce the magnitude of $F_p r$ from the actual in-place value. The normalized form is termed the overconsolidation ratio (OCR) and defined by:

$$OCR = F_p r / F_{vo} r \tag{9-16}$$

Soils are often overconsolidated to some degree because they are old in geologic time scales and have undergone many changes. Mechanisms causing overconsolidation include erosion, desiccation, groundwater fluctuations, aging, freeze-thaw cycles, wet-dry cycles, glaciation, and cementation.

A representative *e-log($F_v r$)* curve obtained from one-dimensional consolidation testing on a marine clay is presented in Figure 9-17. The observed preconsolidation stress is seen to separate the recompression phase ("elastic strains") from the virgin compression portion (primarily "plastic strains") of the response.

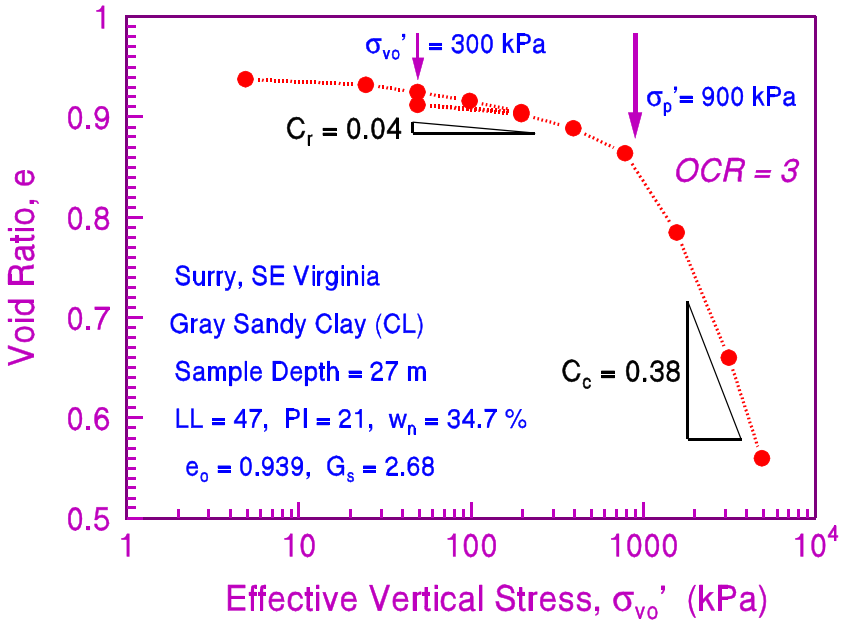

Figure 9-17. Representative Consolidation Test Results in Overconsolidated Clay

A check on the reasonableness of the obtained compression indices may be afforded via empirical relationships with the plasticity characteristics of the clay. A long-standing expression for the compression index (C_c) in terms of the liquid limit (LL) is given by (Terzaghi, et al., 1996):

$$C_c = 0.009\,(LL-10) \tag{9-17}$$

In natural deposits, the measured C_c may be greater than that given by (9-17) because of inherent fabric, structure, and sensitivity. For example, in the case in Fig. 9-17 with LL = 47, (9-17) gives a calculated C_c = 0.33 vs. measured C_c = 0.38 in the oedometer.

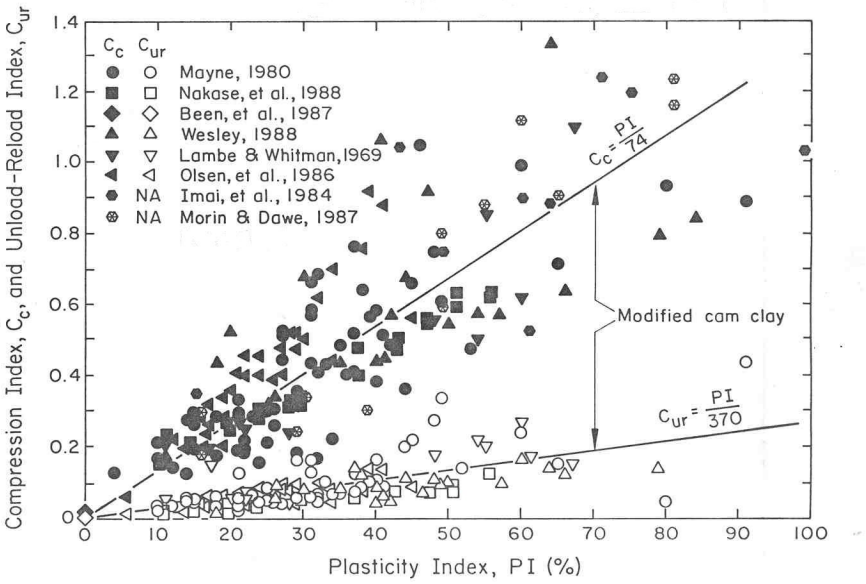

Figure 9-18. Trends for Compression and Swelling Indices in Terms of Plasticity Index.

Statistical expressions for the virgin compression index (C_c) and the swelling index (C_s) from unload-reload cycles are given in Figure 9-18 in relation to the plasticity index (PI). However, it should be noted that the PI is obtained on remolded soil, while the consolidation indices are measurements on natural clays and silts. Thus, structured soils with moderate to high sensitivity and cementation will depart from these observed trends and signify that additional testing and care are warranted.

In clays and silts, the profile of preconsolidation stress can be evaluated via in-situ test data. A relationship between $F_p r$, plasticity index (PI) and the (raw) measured vane strength (s_{uv}) is given in Figure 9-19. This permits immediate assessment of the degree of overconsolidation of natural soil deposits.

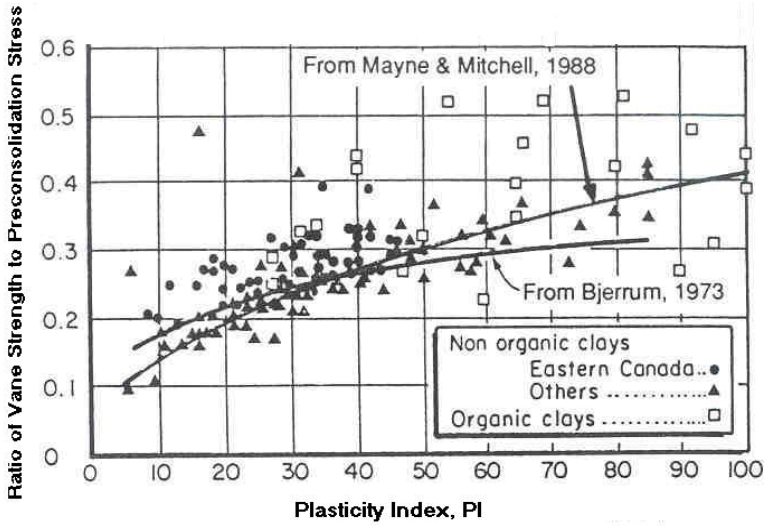

Figure 9-19. Ratio of Measured Vane Strength to Preconsolidation Stress ($s_{uv}/F_p r$) vs. Plasticity Index (I_p) (after Leroueil and Jamiolkowski, 1991).

For the electric cone penetrometer, Figure 9-20 shows a relationship for $F_p r$ in terms of net cone tip resistatnce (q_T-F_{vo}) for intact clay deposits. Fissured clays are seen to lie above this trend. For the piezocone, $F_p r$ can be evaluated from excess porewater pressures (u_1-u_0), as seen in Figure 9-21.

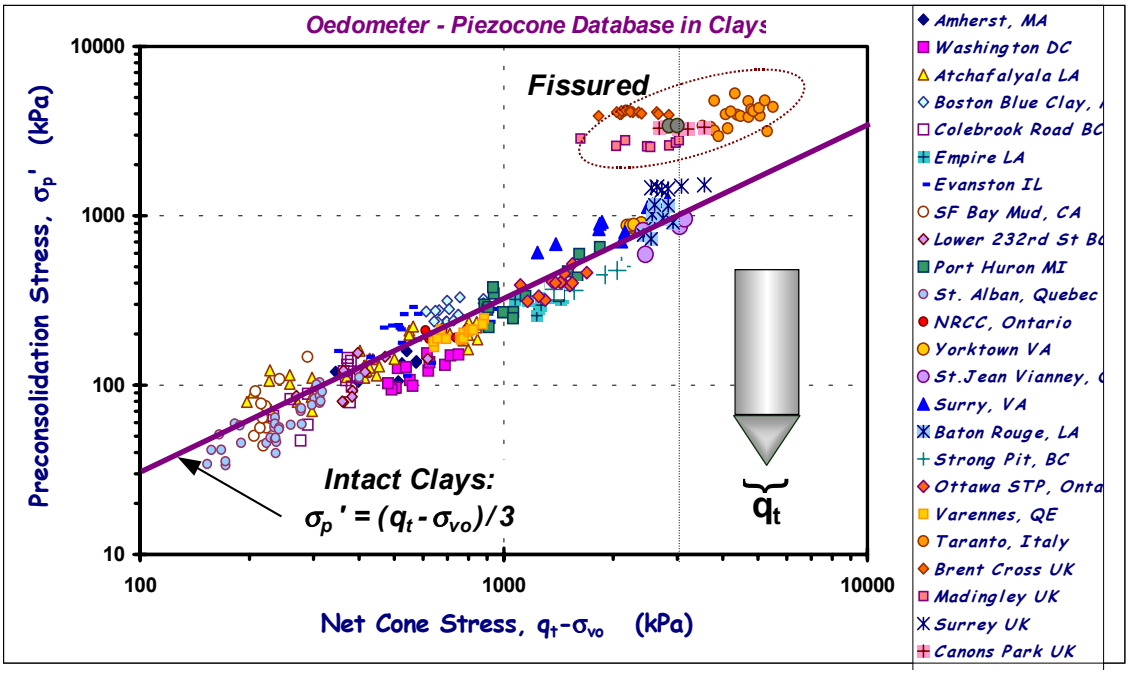

Figure 9-20. Preconsolidation Stress Relationship with Net Cone Tip Resistance from Electrical CPT.

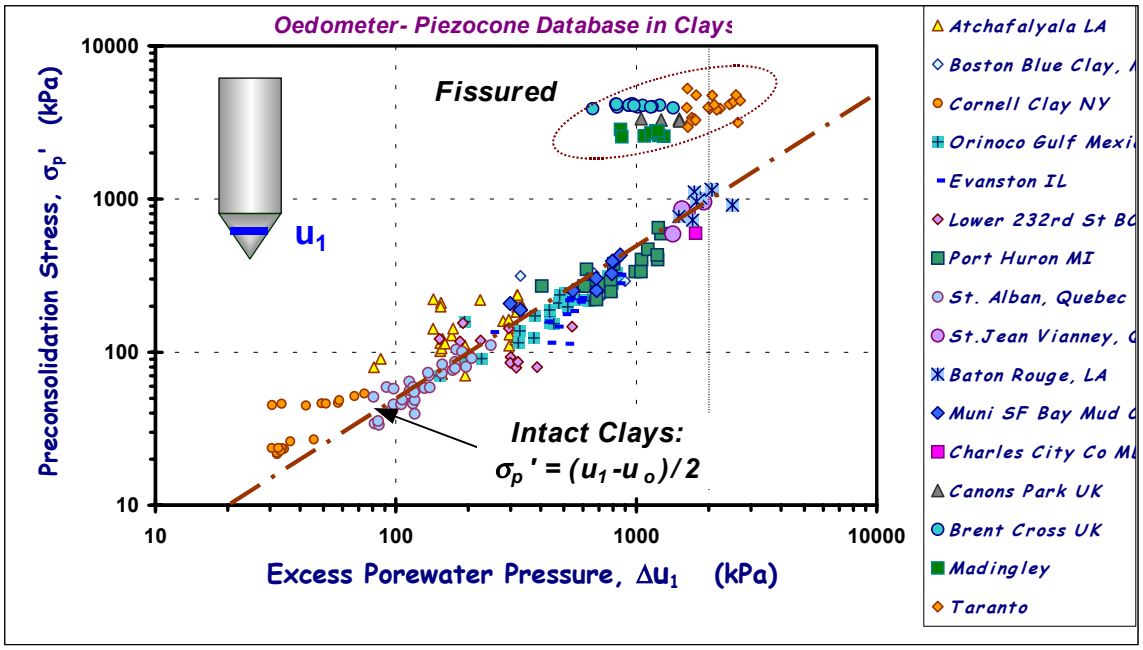

Figure 9-21. Relationship Between Preconsolidation Stress and Excess Porewater Pressures from Piezocones.

A direct correlation between the effective preconsolidation stress and effective contact pressure (p_0-u_0) measured by the flat dilatometer is given in Figure 9-22, again noting that intact clays and fissured clays respond differently. The shear wave velocity (V_S) can also provide estimates of $F_P r$, per Figure 9-23. In all cases, profiles of $F_p r$ obtained by in-situ tests should be confirmed by discrete oedometer results.

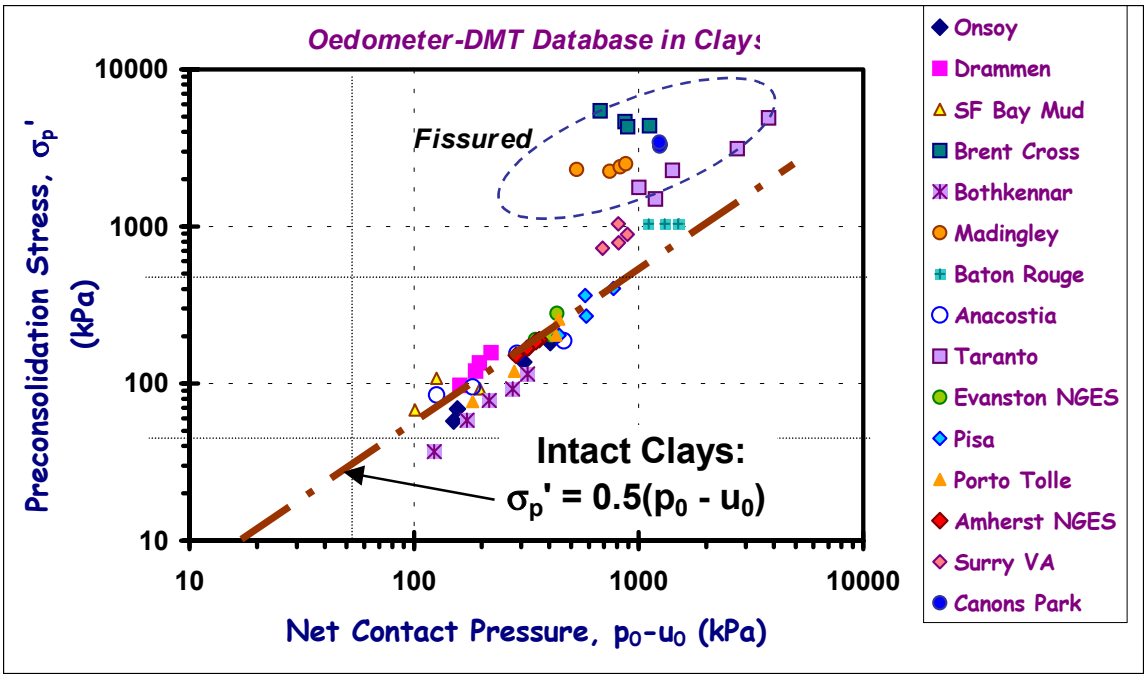

Figure 9-22. Relationship Between Preconsolidation Stress and DMT Effective Contact Pressure in Clays.

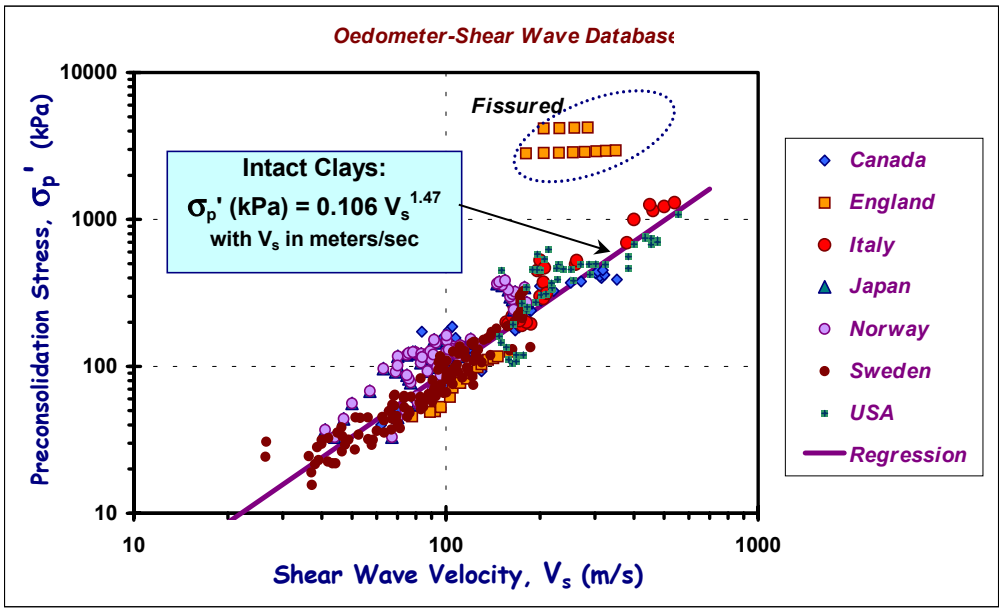

Figure 9-23. Relationship Between Preconsolidation Stress and Shear Wave Velocity in Clays.
(Data from Mayne, Robertson, & Lunne, 1998)

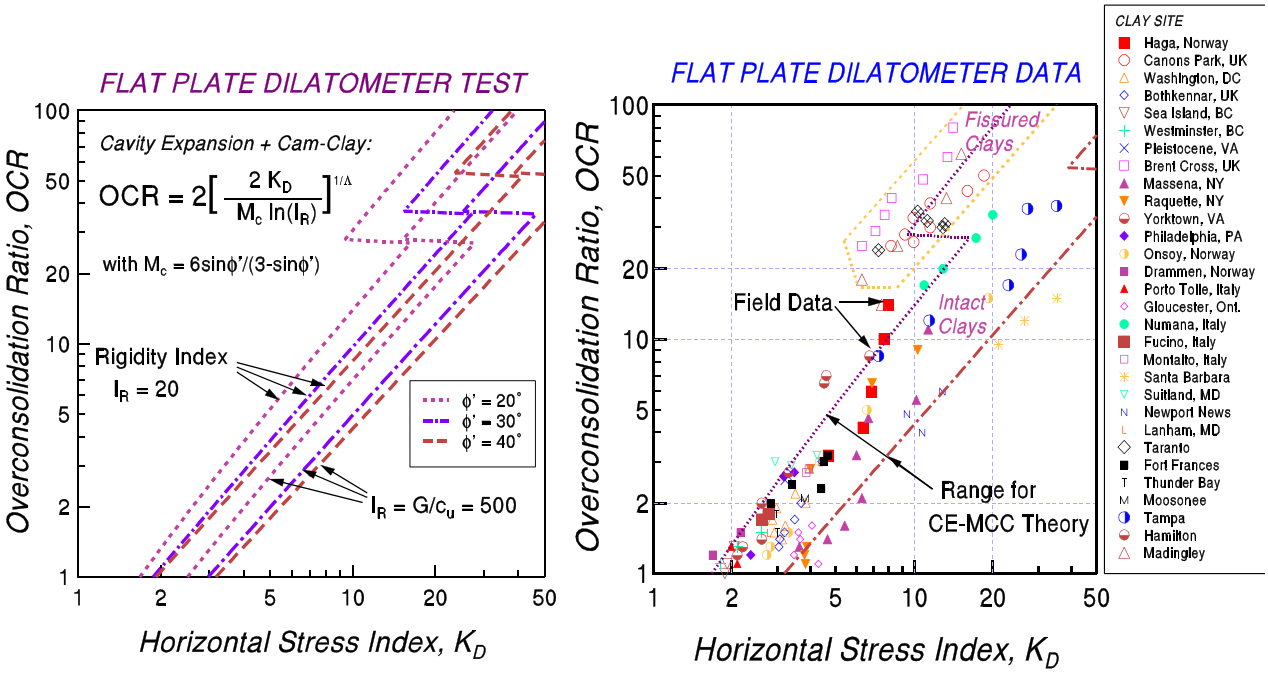

Figure 9-24. Relationships Between Overconsolidation Ratio and DMT Horizontal Stress Index, K_D from (a) Cavity Expansion-Critical State Theory, and (b) Worldwide Database from Clays.

The stress history can also be expressed in terms of a dimensionless parameter, the overconsolidation ratio, OCR = $F_p r/F_{vo} r$. For the flat dilatometer test (DMT), the OCR can be theoretically related to the horizontal stress index [$K_D = (p_0-u_0)/F_{vo} r$] using a hybrid formulation based on cavity expansion and critical state soil mechanics, as shown in Figure 9-24a (Mayne, 2001). The relationship is not a singular expression between OCR and K_D , as has been suggested earlier (e.g., Marchetti, 1980; Schmertmann, 1986) but also depends on other clay properties and parameters, including the effective stress friction angle (Nr), plastic volumetric strain ratio, (7), and the undrained rigidity index, $I_R = G/s_u$, where G = shear modulus and s_u = undrained shear strength. The parameter 7 . 1 - C_s/C_c, where C_s = swelling index and C_c = virgin compression index, as obtained from one dimensional consolidation test results (Chapter 6). The parameter Mc is used to represent the frictional characteristics: $M_c = 6 \sin Nr/(3-\sin Nr)$. The relationship between OCR and K_D may also depend upon other variables that have not yet been incorporated into the expression, including the age of the deposit, its fabric, structure, and minerology.

An important facet is whether the clay is intact or fissured. Fissuring can be caused by excessive unloading (erosion) until passive earth pressure conditions are invoked, or by extensive desiccation and other mechanisms. The degree of fissuring effectively reduces the operational strength of the clay. Consequently, when the limiting OCR has been reached (see Section 9.4.4), the above expression in Figure 9-24a has been adjusted to reflect an operational shear strength (s_u) reduced to one-half its value for intact clays.

Compiled data from clays tested worldwide are presented in Figure 9-24b to show the general trend between OCR and K_D. The boundaries from the *Cavity Expansion-Modified Cam Clay* (CE-MCC) evaluations are superimposed to show the data fall within these ranges. In addition, using expected mean values of soil parameters (Nr = 30°, 7 = 0.8, I_R = 100), results in the expression: OCR = $(0.63\ K_D)^{1.25}$ which is rather similar to the original and singular equation suggested by Marchetti (1980): OCR = $(0.50\ K_D)^{1.56}$.

A similar approach for obtaining the OCR from piezocone test results in clays is shown in Figure 9-25, using a formulation based on CE-MCC concepts (Mayne, 1991). In this case, two separate measurements are utilized from the piezocone data (q_T and u_2), thus reducing the number of input parameters needed in the expression. Consequently, the overconsolidation ratio is related to the normalized piezocone parameter, $(q_T - u_2)/F_{vo}r$, as well as the parameters $M_c = 6 \sin Nr/(3-\sin Nr)$ and $7 \ . \ 1 - C_s/C_c$.

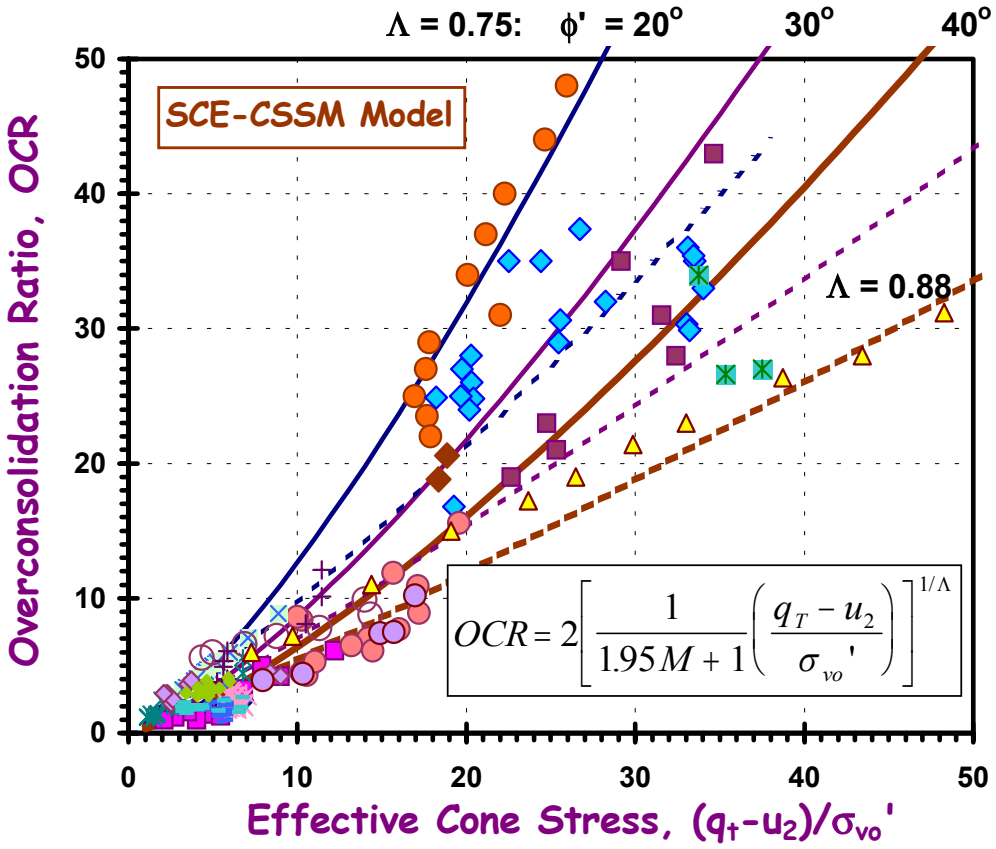

Figure 9-25. Summary Calibrations of OCR Evaluations Using Piezocone Results in Clays with Superimposed Curves from Analytical Model.

9.4.3. Undrained Strength of Clays & Silts

The undrained shear strength (s_u or c_u) is not a unique property of soils, but a behavioral response to loading that depends upon applied stress direction, boundary conditions, strain rate, overconsolidation, degree of fissuring, and other factors. Therefore, it is often a difficult task to directly compare undrained strengths measured by a variety of different lab and field tests, unless proper accounting of these factors is given due consideration and adjustments are made accordingly. For example, the undrained shear strength represents the failure condition corresponding to the peak of the shear stress vs. shear strain curve. The time to reach the peak is a rate effect, such that consolidated undrained triaxial tests are usually conducted with a time-to-failure on the order of several hours, whereas a vane shear may take several minutes, yet in contrast to seconds by a cone penetrometer.

The direction of loading has a marked influence on the measured undrained strength (e.g., Jamiolkowski, et al., 1985) and this facet is known as *strength anisotropy*. The undrained strength corresponding to horizontal loading of clays (termed extension-type loading or passive mode) is less than that under vertical loading (compression or active mode). The mode of simple shear is an intermediate value and corresponds to a representative average undrained shear strength for routine design purposes (Ladd, 1991).

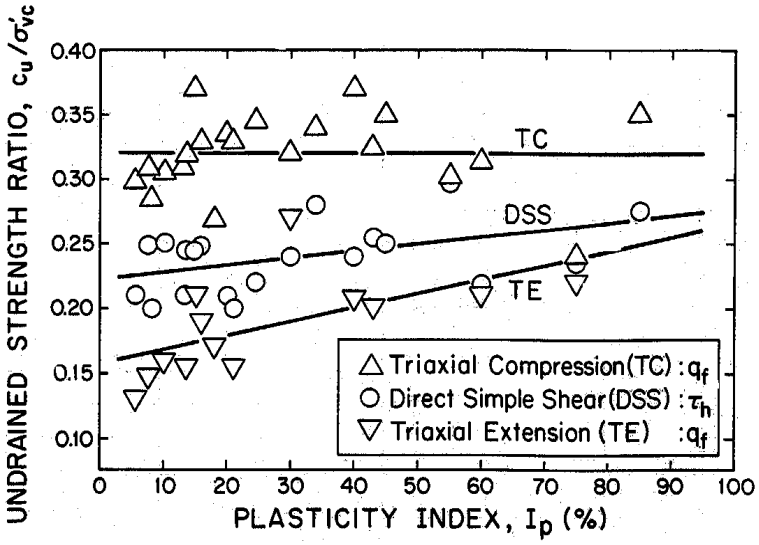

Since most commercial and governmental laboratories are not equipped to run series of triaxial compression (TC), direct simple shear (DSS), and triaxial extension (TE) tests, either empirical or constitutive relationships may be employed. For normally-consolidated clays & silts, Figure 9-26 shows the relative hierarchy of these modes and the observed trends with plasticity index (I_p). In this presentation, the undrained shear strength has been normalized by the effective overburden stress level, as denoted by the ratio ($s_u/F_{vo}r$,or $c_u/F_{vo}r$), that refers to the older c/pr ratio.

Figure 9-26. Modes of Undrained Shear Strength Ratio $(s_u/F_{vo}r)_{NC}$ for Normally-Consolidated Clays (Jamiolkowski, et al. (1985).

The theoretical interrelationships of undrained loading modes for normally-consolidated clay are depicted in Figure 9-27 using a constitutive model (Ohta, et al., 1985). The ratio for normally consolidated clay $(s_u/F_{vo}r)_{NC}$ increases with Nr for each of the shearing modes, including isotropically-consolidated triaxial compression (CIUC), plane strain compression (PSC), anisotropically-consolidated triaxial compression (CK_0UC), shear box test (SBT), direct simple shear (DSS), pressuremeter (PMT), vane shear (VST), plane strain extension (PSE), and anisotropically-consolidated triaxial extension test (CK_0UE). Laboratory data from 206 clays confirm the general nature of these relations (Kulhawy & Mayne, 1990).

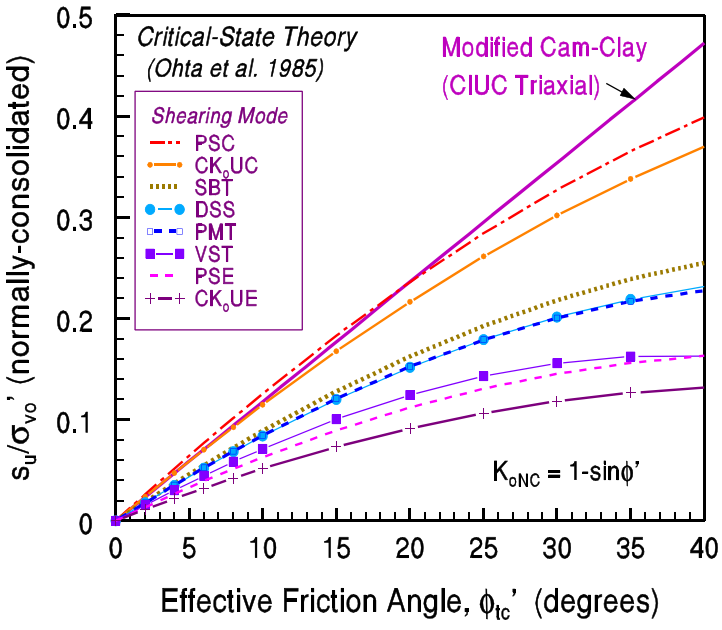

Figure 9-27. Normalized Undrained Strengths for NC Clay Under Different Loading Modes by Constitutive Model (Ohta, et al., 1985).

Based on extensive experimental data (Ladd, 1991) and critical state soil mechanics (Wroth, 1984), the ratio $(s_u/F_{vo}r)$ increases with overconsolidation ratio (OCR) according to:

$$(s_u/F_{vo}r)_{OC} = (s_u/F_{vo}r)_{NC}\ OCR^{\Lambda} \qquad (9\text{-}18)$$

where Λ . 1- C_s/C_c and generally taken to be about 0.8 for unstructured and uncemented soils. Thus, if a particular shearing mode is required, it can be assessed using either Figures 9-26 or 9-27 to obtain the NC value and equation (9-17) to determine the undrained strength for overconsolidated states. In many situations involving embankment stability analyses and bearing capacity calculations, the simple shear mode may be considered an average and representative value of the undrained strength characteristics, as shown by Figure 9-28 and given by:

$$(s_u/F_{vo}r)_{DSS} = \tfrac{1}{2} \sin Nr\ OCR^{\Lambda} \qquad (9\text{-}19)$$

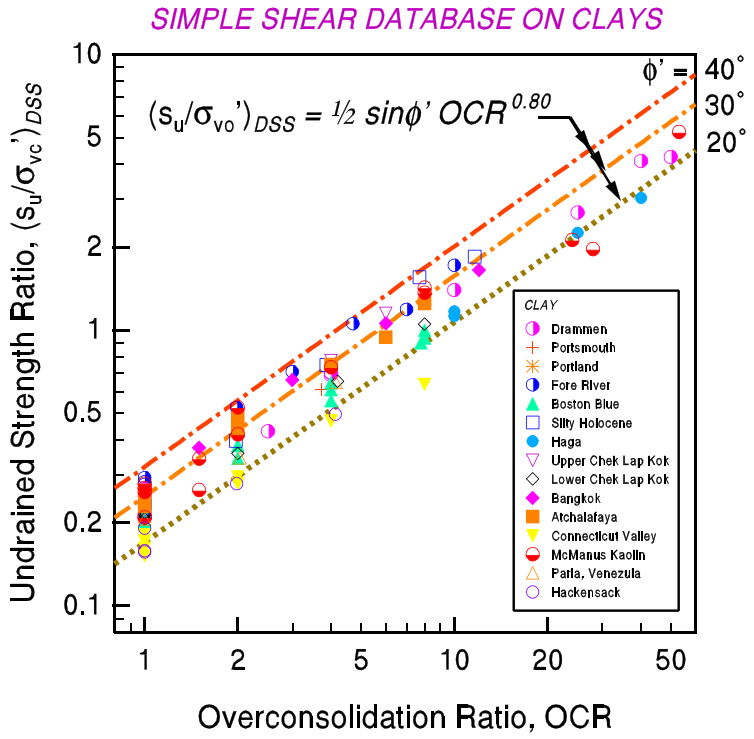

Figure 9-28. Undrained Strength Ratio Relationship with OCR and Nr for Simple Shear Mode.

For intact soft clays and silts at low OCRs < 2, equation (9-18) reduces to the simple form (Nr = 30°):

$$s_u\ (DSS)\ .\ 0.22\ F_p\ r \qquad (9\text{-}20)$$

which is consistent with backcalculated strengths from failures of embankments, footings, and excavations, as well as the correction of vane shear strengths measured in-situ (Terzaghi, et al. 1996). Projects involving soft ground construction should utilized equation (9-19) in evaluating the mobilized undrained shear strength for design (Jamiolkowski, et al., 1985; Ladd, 1991).

9.4.4. Lateral Stress State

The lateral geostatic state of stress (K_0) is one of the most elusive measurements in geotechnical engineering. It is often represented as the coefficient of horizontal stress $K_0 = F_{ho}r / F_{vo}r$ where $F_{ho}r$ = effective lateral stress and $F_{vo}r$ = effective vertical stress. A number of innovative devices have been devised to measure the in-place total horizontal stress (F_{ho}) including: total stress cell (push-in spade), self-boring pressuremeter, hydraulic fracturing apparatus, and the Iowa stepped blade. Recent research efforts attempt to use sets of directionalized shear wave measurements to decipher the in-situ K_0 in soil formations.

For practical use, it is common to relate the K_0 state to the degree of overconsolidation, such as:

$$K_0 = (1 - \sin Nr)\, OCR^{\sin Nr} \qquad (9\text{-}21)$$

which was developed on the basis of special laboratory tests including instrumented oedometer tests, triaxial cells, and split rings (Mayne & Kulhawy, 1982). Figure 9-29 shows the general applicability of (9-20) compared with direct field data measurements of K_0 for clays and sands.

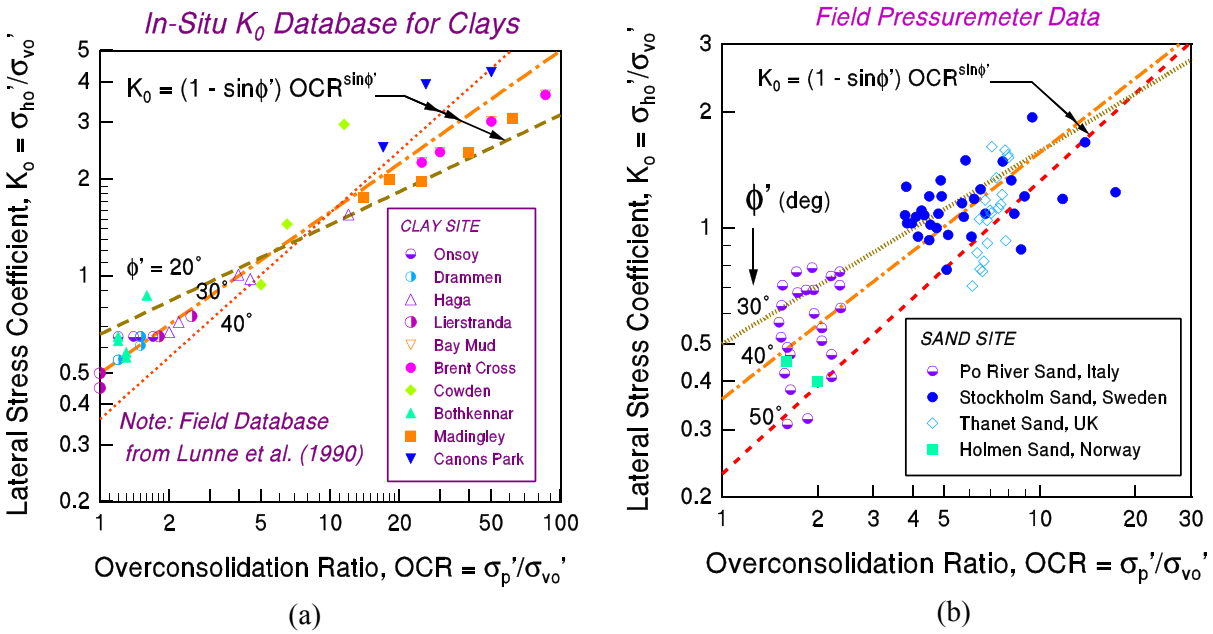

Figure 9-29. Field K_0 - OCR Relationships for (a) Natural Clays and (b) Natural Sands.

In general, the value of K_0 has an upper bound value limited by the passive coefficient, K_p. The simple Rankine value is given by:

$$K_p = \tan^2 (45° + \tfrac{1}{2}\, Nr) = (1+\sin Nr)/(1-\sin Nr) \qquad (9\text{-}22)$$

When the in-situ K_0 reaches the passive value K_p, fissures and cracks can develop within the soil mass. This can be important in sloped masses since extensive fissuring is often associated with drained strengths that are at or near the residual strength parameters ($N_r r$ and $c_r r = 0$). In desiccated clays, fissuring can occur before the passive earth pressures are reached. In cemented materials, a value of K_p in excess of (9-22) can be achieved if bonding exists, such that: $K_p = N_N + 2cr/F_{vo}r$ %&N_N where $N_N = (1+\sin Nr)/(1-\sin Nr)$.

A limiting value of OCR can be defined when (9-21) equals (9-22):

$$OCR_{limit} = \left[\frac{(1+\sin\phi')}{(1-\sin\phi')^2} \right]^{(1/\sin\phi')} \tag{9-22}$$

A network of fissures in the deposit can effectively reduce the operational undrained shear strength of the clay. Thus, the OCR_{limit} can be used to place upper bounds on calculated s_u values given by equations (9-18) and (9-19), as well as set upper bounds for K_0 given by (9-21).

For evaluating K_0 in clays, it is recommended that (9-21) be used in conjunction with the profile of OCR determined from oedometer tests and supplemented with the in-situ correlations given in Section 9.4.2. Triaxial or direct shear testing can be used to provide the relevant Nr of the material. The flat dilatometer test (DMT) has also been used for directly assessing K_0 in-situ for clays, silts, and sands, and a comprehensive review of the available relationships is given by Mayne & Martin (1998).

For the determination of K_0 in clean quartz sands by CPT, a calibration chamber database has been compiled and analyzed (Lunne, et al., 1997). The results have been based on statistical multiple regression studies of 26 separate sands worldwide where boundary effects of the chamber sizes were considered (Kulhawy & Mayne, 1990). Each flexible-walled calibration chamber was between 0.9 and 1.5 m in diameter with height of same magnitude. Preparation of a sand deposit in these large chambers takes approximately one week by pluviation or slurry methods. Relative densities range from about 10 % to almost 100 %. After placement, the sample is subjected to one of a variety of stress conditions using applied vertical and horizontal stresses and normally-consolidated to overconsolidated states (1 # OCRs # 15). Tests are usually dry or saturated, with or without back pressures. The final phase is the conduct of the CPT through the center of the cylindrical specimen. The summary results of the chamber test database are presented in Figure 9-30 indicating a relationship between the applied lateral stress and measured cone tip stress.

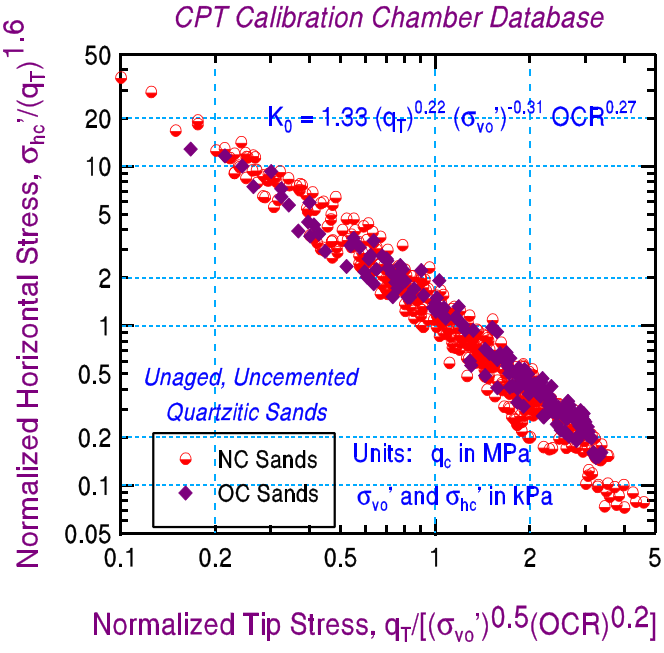

Figure 9-30. Relationship for Lateral Stress State Determination in Sands from CPT.

Combining the expression from Figure 9-30 with equation (9-21), an estimate of the overconsolidation ratio of the sand can be made (Mayne, 1995, 2001):

$$OCR = \left[\frac{1.33}{K_{oNC}} \frac{q_T^{0.22}}{(\sigma_{vo}')^{0.31}} \right]^{1/(\alpha - 0.27)} \qquad (9\text{-}23)$$

where $K_{oNC} = 1\text{-}\sin\phi$ and $\alpha = \sin\phi$.

9.5. STIFFNESS AND DEFORMATION PARAMETERS

The stiffness of soils is represented by several parameters, including consolidation indices (C_c, C_r, C_s), drained moduli (E, G, K, D), undrained moduli (E_u, G_u), and and/or subgrade reaction coefficient (k_s). The elastic constants are defined as per Figure 9-30. For undrained loading, no volume change occurs ($\Delta V/V = 0$), while for drained loading, volumetric changes can be contractive (decrease) or dilative (increase). In some manner, all of the deformation parameters are interrelated (usually via elastic theory). For example, the recompression index (C_r), which is often taken equal to the swelling index (C_s), can be related to the constrained modulus ($D = \Delta\sigma_v/\Delta\varepsilon_v$) obtained from consolidation tests:

$$D = [(1+e_0)/C_r] \ln(10)\, \sigma_{vo}' \qquad (9\text{-}24)$$

which is valid for the overconsolidated portion only. When the imposed embankment loading exceeds the preconsolidation stress of the underlying natural clay such that the soil becomes normally-consolidated, the corresponding D would utilize C_c in equation (9-24)

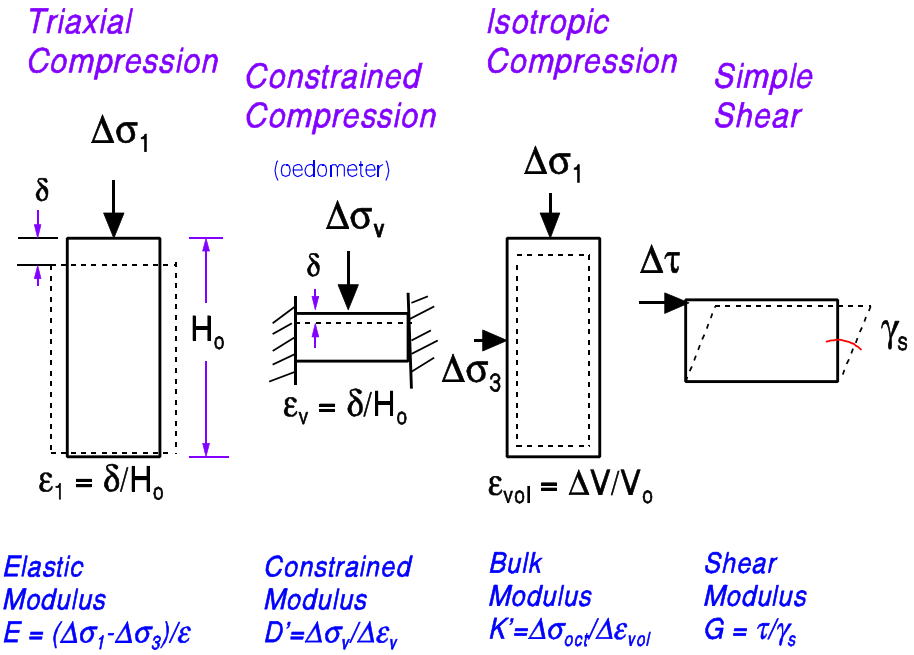

Figure 9-31. Definitions of Elastic Moduli in Terms of Loading & Applied Boundary Conditions.

The drained moduli are interrelated by the following expressions (Lambe & Whitman, 1979):

$$Er = 2\,Gr\,(1 + <r) \tag{9-25}$$

$$Dr = Er\,(1- <r)\,/[(1 + <r)(1- 2\,<r)] \tag{9-26}$$

$$Kr = Er/[3(1- 2\,<r)] \tag{9-27}$$

where $<r$. 0.2 is the drained Poisson's ratio for all types of geomaterials (Tatsuoka & Shibuya, 1992). For undrained loading, the equivalent Poisson's ratio is $<_u$. 0.5, and therefore the relationship between Young's modulus and shear modulus becomes:

$$E_u = 3\,G_u \tag{9-28}$$

Note that the constrained modulus and bulk modulus are not applicable for undrained conditions.

Certain in-situ tests attempt to measure the deformation characteristics of soils directly in place, including the pressuremeter, flat dilatometer, plate load test, and screw plate. In fact, elastic theory is usually invoked for these tests to determine an equivalent elastic modulus (E). However, major difficulties occur in assessing the appropriate magnitude of modulus due to the degree of disturbance caused during installation, degree of drainage, and corresponding level of strains imposed, particularly since the stress-strain-strength behavior of soils is nonlinear, anisotropic, and strain-rate dependent. That is, modulus is a non-singular value that varies with stress level, strain, and loading rate. In many geotechnical investigations, only the results of SPT and/or CPT are available, yet an assessment of deformation parameters is needed for settlement analyses and calculations of deflections. The penetration data reflect measurements taken late in the stress-strain response, corresponding to the strength of the material, as implicated by Figure 9-31.

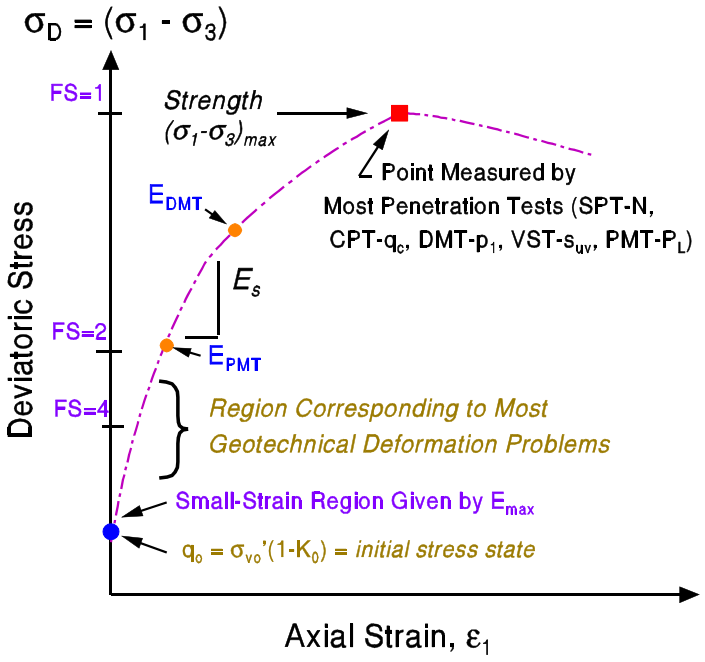

Figure 9-32. Idealized Stress-Strain Curve and Stiffnesses of Soils at Small- and Large-Strains.

The PMT and DMT provide data earlier in the stress-strain curve, yet perhaps often beyond the values of interest, unless unload-reload measurements are taken to better define an equivalent elastic region. Corresponding factors of safety (FS) from initial stress state (K_o) to failure (J_{max}) can be associated with the moduli, as shown in Figure 9-31. The initial stiffness is represented by the nondestructive value obtained from the shear wave velocity and provides a clear benchmark value.

9.5.1. Small-Strain Modulus

Recent research outside of the U.S. has found that the small-strain stiffness from shear wave velocity (V_s) measurements applies to the initial static monotonic loading, as well as the dynamic loading of geomaterials (Burland, 1989; Tatsuoka & Shibuya, 1992; LoPresti et al., 1993). Thus, the original dynamic shear modulus (G_{dyn}) has been re-termed the maximum shear modulus (now designated G_{max} or G_0) that provides an upper limit stiffness given by: $G_0 = D_T V_s^2$ where $D_T = (_T/g$ = total mass density of the soil, $(_T$ = total unit weight (saturated value can be obtained from Fig. 9-5), and g = 9.8 m/s^2 = gravitational constant. This G_0 is a fundamental stiffness of all solids in civil engineering and can be measured in all soil types from colloids, clays, silts, sands, gravels, boulders, to fractured and intact rocks. The corresponding equivalent elastic modulus is found from: $E_{max} = E_0 = 2G_0 (1+<)$ where < = 0.2 is a representative value of Poisson's ratio of geomaterials at small strains. Shear waves can be measured by both field techniques (Section 5.7) and laboratory methods (see Figures 7-12 and 7-13).

In certain geologic materials, it has been possible to develop calibrated correlations between specific tests (e.g., PMT, DMT) and performance monitored data from full-scale foundations and embankments. These tests provide a modulus intermediate along the stress-strain-strength curve (Fig. 9-32). Of particular note, the small-strain modulus from shear wave velocity measurements provides an excellent reference value, as this is the maximum stiffness of the soil at a given void ratio and effective confining state. Herein, a generalized approach based on the small strain stiffness from shear wave measurements will be discussed, whereby the initial modulus (E_0) is reduced to an appropriate stress level for the desired FS.

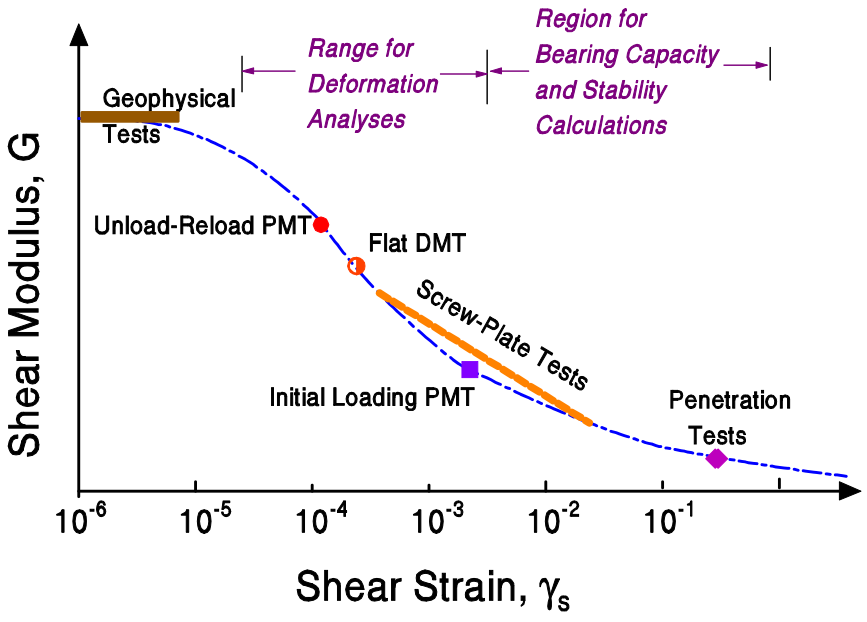

Figure 9-33. Conceptual Variation of Shear Modulus with Strain Level Under Static Monotonic Loading and Relevance to In-Situ Tests.

9.5.2. Modulus Reduction

Shear modulus reduction with shear strain is often shown in normalized form, with the corresponding G divided by the maximum G_{max} (or G_0). The relationship between G/G_0 and logarithm of shear strain is well recognized for dynamic loading conditions (e.g., Vucetic and Dobry, 1991), however, the monotonic static loading shows a more severe decay with strain, as seen in Figure 9-33. The cyclic curve is representative resonant column test results, whereas the monotonic response has been only recently observed by special internal & local strain measurements in triaxial and torsional tests (e.g., Tatsuoka & Shibuya, 1992; Jamiolkowski, et al. 1994).

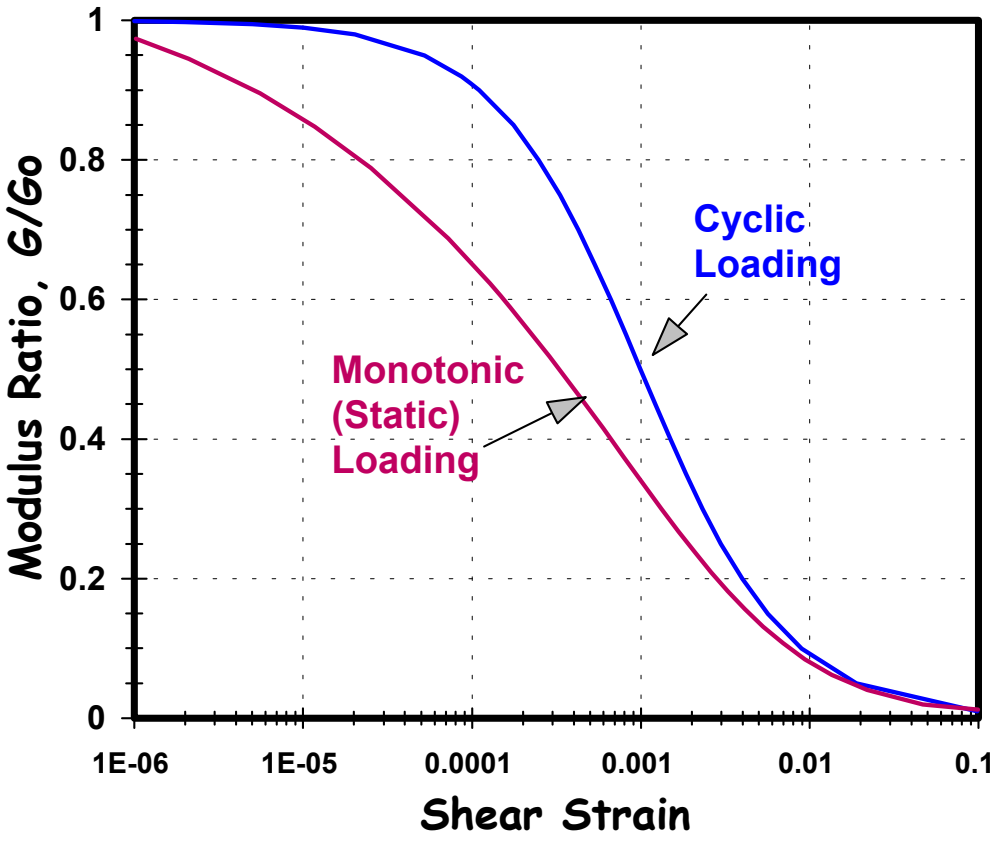

Figure 9-34. Modulus Reduction with Log Shear Strain for Initial Monotonic (Static) and Dynamic (Cyclic) Loading Conditions.

An alternate means of presenting modulus reduction is terms of shear stress level. Figure 9-34 shows a selection of normalized secant moduli (E/E_0) with varying stress level (q/q_{ult}) obtained from laboratory tests on uncemented, unstructured sands and clays. The stress level is expressed as J/J_{max} or q/q_{ult},where $J = q = \frac{1}{2}(F_1-F_3)$ = shear stress and $J_{max} = q_{ult}$ = the shear strength. The laboratory monotonic shear tests have been performed under triaxial and torsional shear conditions with local internal strain instrumentation to allow measurements spanning from small- to intermediate- to large-strain response (LoPresti, et al. 1993, 1995; Tatsuoka & Shibuya, 1992).

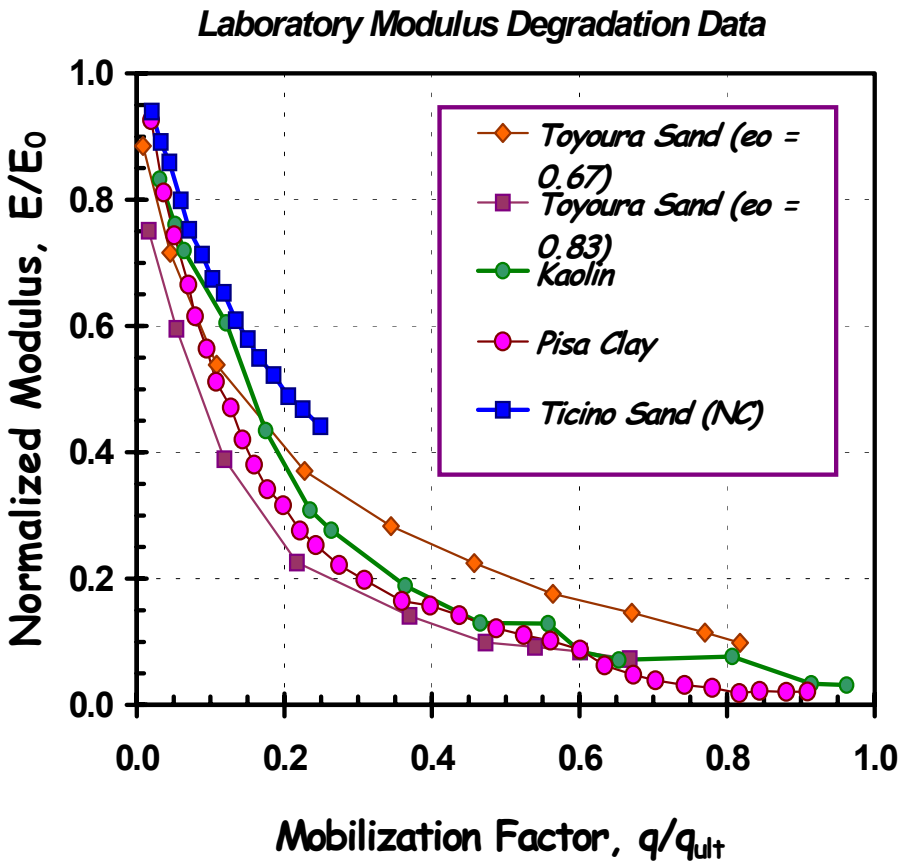

Figure 9-35. Modulus Degradation from Instrumented Laboratory Tests on Uncemented and Unstructured Geomaterials.

A modified hyperbola can be used as a simple means to reduce the small-strain stiffness (E_0) to secant values of E at working load levels, in terms of mobilized strength (q/q_{ult}). Figure 9-35 illustrates the suggested trends for unstructured clays and uncemented sands. The generalized form may be given as (Fahey & Carter, 1993):

$$E/E_0 = 1 - f\,(q/q_{ult})^g \qquad (9\text{-}29)$$

where f and g are fitting parameters. Values of $f = 1$ and $g = 0.3$ appear reasonable first-order estimates for unstructured and uncemented geomaterials (Mayne, et al. 1999a) and these provide a best fit for the measured data shown before in Figure 9-34. The mobilized stress level can also be considered as the reciprocal of the factor of safety, or $(q/q_{ult}) = 1/FS$. That is, for $(q/q_{ult}) = 0.5$, the corresponding FS = 2.

Other numerical forms for modulus degradation are available (e.g., Duncan & Chang, 1970; Hardin & Drnevich, 1972; Tatsuoka & Shibuya, 1992) and several have a more fundamental basis or a better fitting over the full range of strains from small- to intermediate- to large-ranges (e.g., Puzrin & Burland, 1998). The intent here, however, is to adopt a simplified approach for facilitating the use of small-strain stiffness data into highway engineering practice.

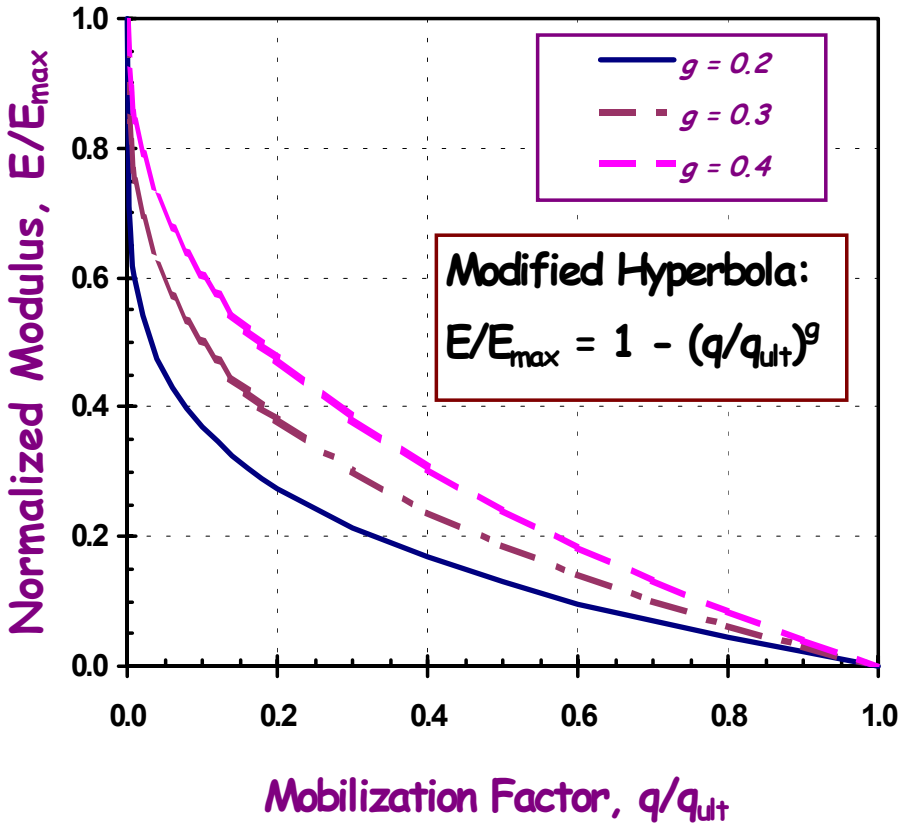

Figure 9-36. Modified Hyperbolas to Illustrate Modulus Degradation Curves (Cases shown for f = 1). Note: Mobilized shear strength = q/q_u = 1/FS, where FS = factor of safety.

9.5.3. Direct and Indirect Assessments of G_0

It is particularly simple and economical to measure shear wave velocity profiles for determination of the small strain stiffness, $E_0 = 2\ G_0\ (1+<r)$, by taking $<r = 0.2$ and $G_0 = D_T\ (V_s)^2$. Several methods previously discussed in Chapter 5.7 include the crosshole (CHT), downhole (DHT), surface wave (SASW), as well as laboratory resonant column test (RCT). The seismic cone (Figure 9-34) and seismic dilatometer offer the advantages of collecting penetration data and geophysical measurements within a single sounding. The results shown in Figure 9-34 from Memphis, TN indicate an optimization of data collection with four independent readings including: tip stress (q_t), sleeve friction (f_s), porewater pressures (u_2), and shear wave velocity (V_s). Additional field methods for V_s profiling are in development and include: downhole suspension logging, seismic refraction, and seismic reflection. Additional lab methods for determining V_s of recent vintage include bender elements and specially-instrumented triaxial and torsional shear devices.

In some cases, direct measurements of G_0 will not be available and its estimation may be required. A series of correlative relationships is given subsequently for the CPT and DMT. These correlations may be used also to check on the reasonableness of acquired data.

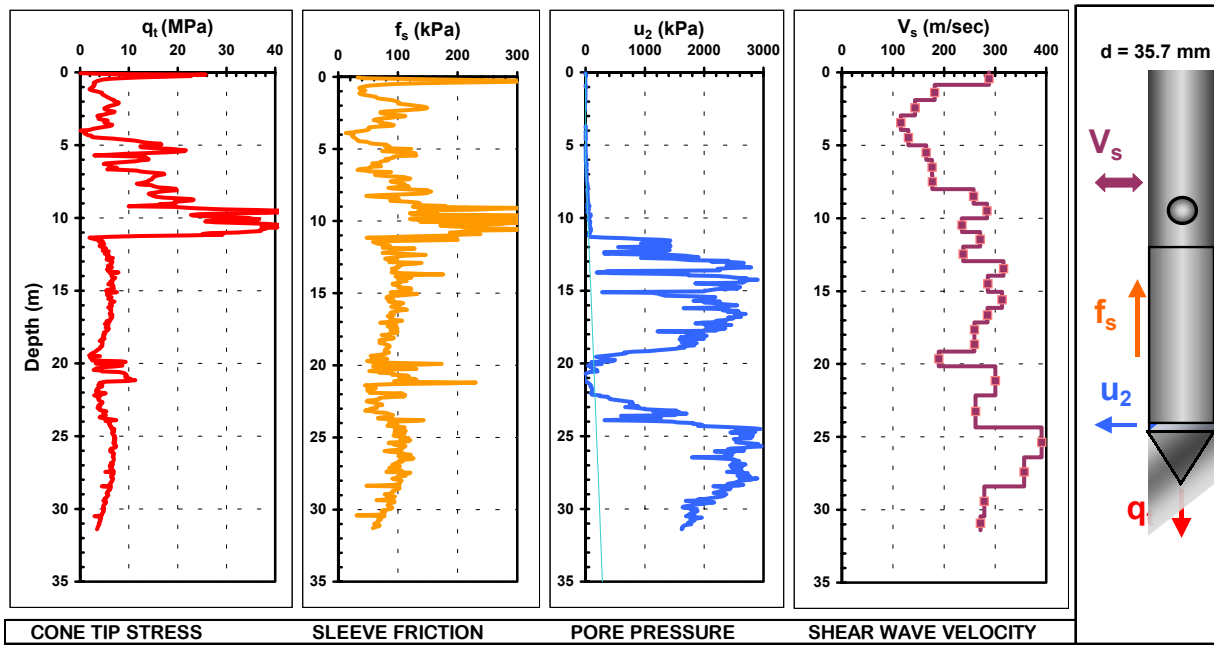

Figure 9-37. Results of Seismic Piezocone Tests (SCPTu) in Layered Soil Profile, Wolf River, Memphis, TN.

The small-strain shear modulus of quartzitic sands may be estimated from the cone tip stress and effective overburden stress, as indicated by Figure 9-35. Similarly, a relationship for obtaining G_0 from DMT in quartz sands is presented in Figure 9-36.

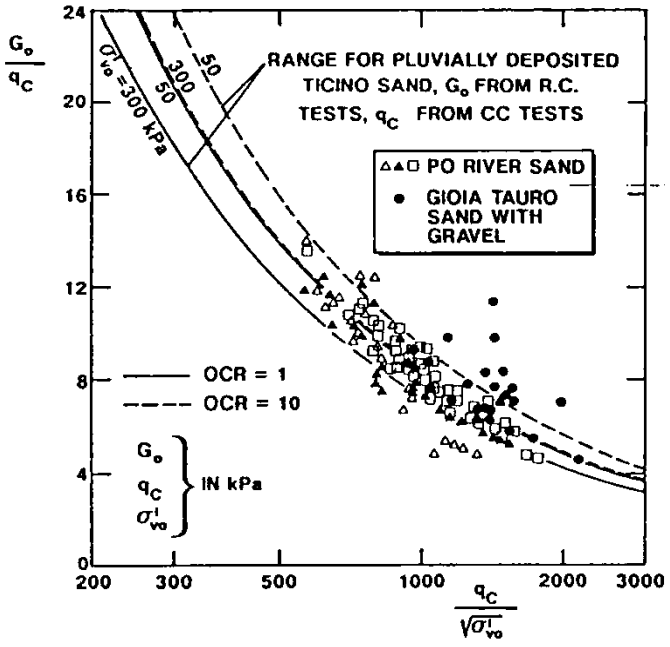

Figure 9-38. Ratio of G_0/q_c with Normalized CPT Resistance for Uncemented Sands (Baldi, et al. 1989).

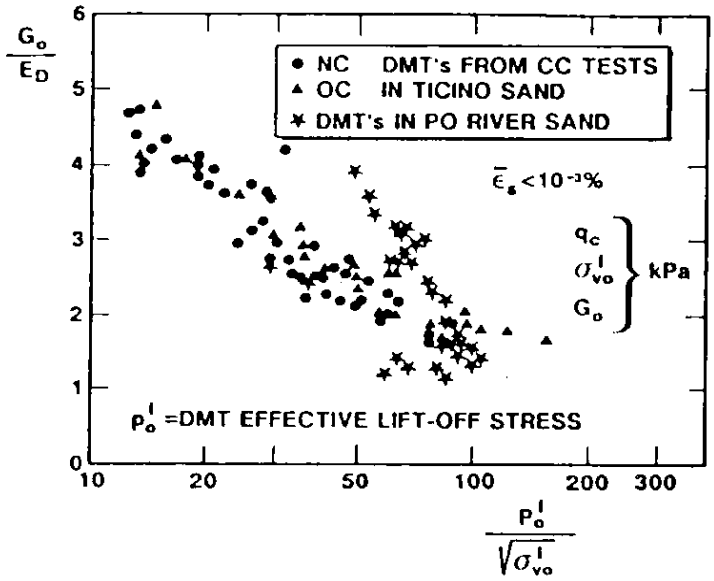

Figure 9-39. Ratio of G_0 /E_D with Normalized DMT Reading for Clean Quartz Sands (Baldi, et al. 1989).

For clays, a relationship between G_0 and corrected tip stress q_T has been noted (Figure 9-37) which also depends upon the inplace void ratio (e_0). Similarly, for the DMT in clays, a trend occurs between G_0 and dilatometer modulus, E_D (Figure 9-38).

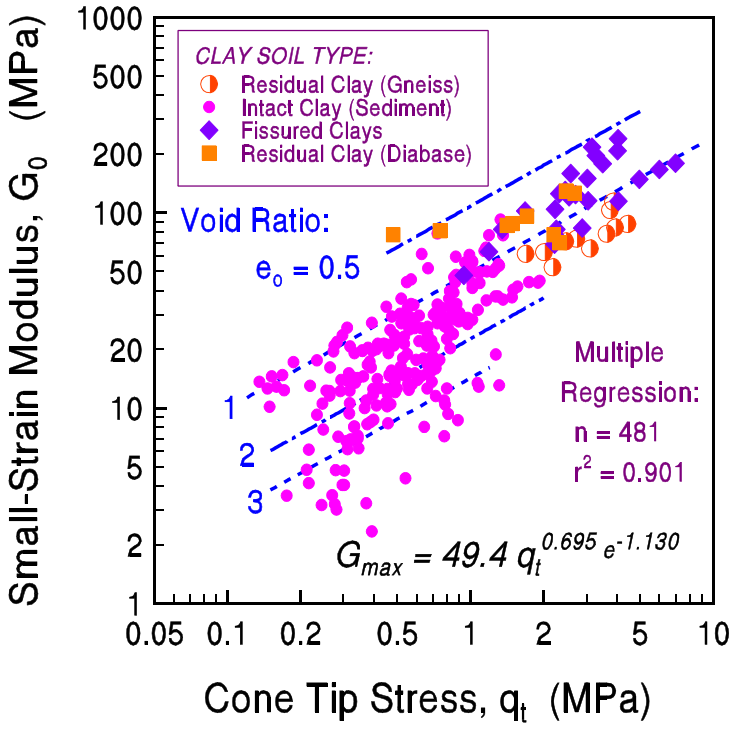

Figure 9-40. Trend Between G_0 and CPT Tip Stress q_T in Clay Soils (Mayne & Rix, 1993).

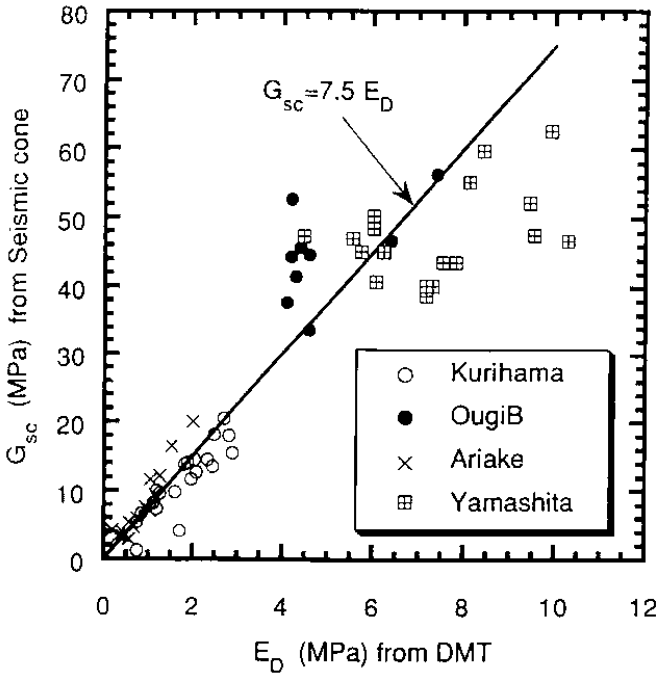

Figure 9-41. Trend Between G_0 and DMT modulus E_D in Clay Soils (Tanaka & Tanaka, 1998).

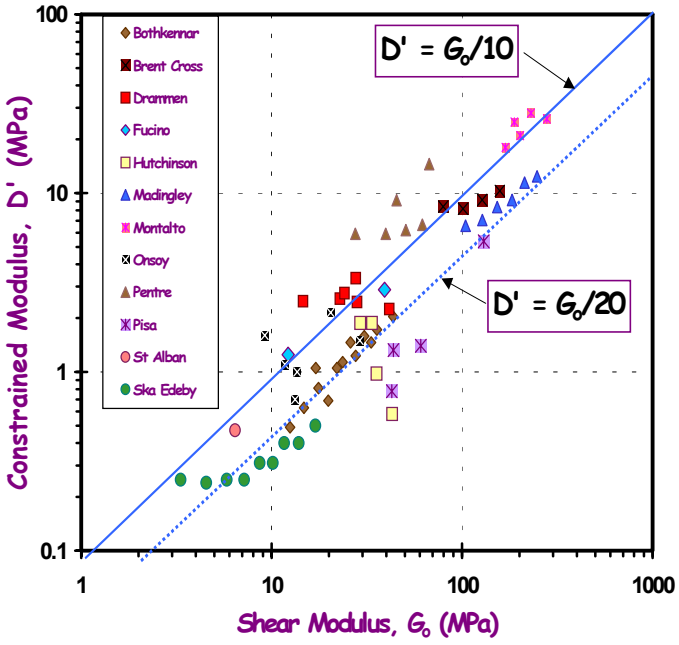

Figure 9-42. Modulus (D') vs. Shear Modulus (G_0) in Clays. Dataset from Burns & Mayne (1998).

In each case, the value of initial shear modulus (G_0) is either directly measured or approximately assessed, and then reduced to the appropriate level of strain or stress by consideration of the relative factor of safety (FS). An alternative would be to directly relate the constrained modulus to the fundamental G_0, such as shown in Figure 9-39 for a wide variety of clays. In these data, all G_0 values were obtained from field measurements using either downhole methods (DHT or SCPTu) or crosshole tests (CHT), or in one case, spectral analysis of surface waves (SASW).

9.6. FLOW PROPERTIES

Soils exhibit flow properties that control hydraulic conductivity (k), rates of consolidation, construction behavior, and drainage characteristics in the ground. Field measurements for soil permeability have been discussed previously in Chapter 6 and include pumping tests with measured drawdown, slug tests, and packer methods. Laboratory methods are presented in Chapter 7 and include falling head and constant head types in permeameters. An indirect assessment of permeability can be made from consolidation test data. Typical permeability values for a range of different soil types are provided in Table 9-1. Results of pressure dissipation readings from piezocone and flat dilatometer and holding tests during pressuremeter testing can be used to determine permeability and the coefficient of consolidation (Jamiolkowski, et al. 1985). Herein, only the piezocone approach will be discussed.

The permeability (k) can be determined from the dissipation test data, either by use of the direct correlative relationship presented earlier (Figure 6-7), or alternatively by the evaluation of the coefficient of consolidation c_h . Assuming radial flow, the horizontal permeability (k_h) is obtained from:

$$k_h = \frac{c_h \gamma_w}{D'} \tag{9-30}$$

where Dr = constrained modulus obtained from oedometer tests.

9.6.1. Monotonic Dissipation

In fine-grained soils, excess porewater pressures ( ) u) are generated during penetration of any probe (pile, cone, blade). For example, in Figure 9-34, large u_2 readings are observed in the clay layer from 11 to 19 m depth. If penetration is halted, the) u will decay eventually to zero (thus the porewater transducer will read the hydrostatic value, u_0). The rate of decay depends on the coefficient of (horizontal) consolidation (c_h) and permeability (k_h) of the medium. An example of piezocone dissipation for both type 1 and 2 filter elements is given in Figure 6-6. These are termed *monotonic* porewater decays because the readings always decrease with time and generally are associated with soft to firm clays and silts. For these cases, the strain path method (Teh & Houlsby, 1991) may be used to determine c_h from the expression:

$$c_h = \frac{T^* a^2 \sqrt{I_R}}{t_{50}} \tag{9-31}$$

where T* = modified time factor from consolidation theory, a = probe radius, $I_R = G/s_u$ = rigidity index of the soil, and t = measured time on the dissipation record (usually taken at 50% equalization).

Several solutions have been presented for the modified time factor T* based on different theories, including cavity expansion, strain path, and dislocation points (Burns & Mayne, 1998). For monotonic dissipation response, the strain path solutions (Teh & Houlsby, 1991) are presented in Figure 9-40(a) and (b) for both midface and shoulder type elements, respectively.

The determination of t_{50} from shoulder porewater decays is illustrated by example in Figure 6-6. For the particular case of 50% consolidation, the respective time factors are T* = 0.118 for the type 1 (midface element) and T* = 0.245 for the type 2 (shoulder element).

TABLE 9-1.

REPRESENTATIVE PERMEABILITY VALUES FOR SOILS

(Modified after Carter and Bentley, 1991)

k = *Hydraulic Conductivity* or *Coefficient of Permeability*	10^{-11}	10^{-10}	10^{-9}	10^{-8}	10^{-7}	10^{-6}	10^{-5}	10^{-4}	10^{-3}	10^{-2}	10^{-1}	1
	meters/sec (m/s)											
	10^{-9}	10^{-8}	10^{-7}	10^{-6}	10^{-5}	10^{-4}	10^{-3}	10^{-2}	10^{-1}	1	10	100
	centimeters/sec (cm/s)											

Permeability:	Practically Impermeable	Very low	Low	Medium	High
Drainage conditions:	Practically Impermeable	Poor	Fair	Good	

Typical soil Groups*:	GC →	GM →		SM	SW →	GW →
	CH	SC	SM-SC MH ML-CL		SP →	GP →

Soil types:	Homogeneous clays below the zone of weathering	Silts, fine sands, silty sands, glacial till, stratified clays	Clean sands, sand and gravel mixtures	Clean gravels
		Fissured and weathered clays and clays modified by the effects of vegetation		

*Note: The arrow adjacent to group classes indicates that permeability values can be greater than the typical value shown.

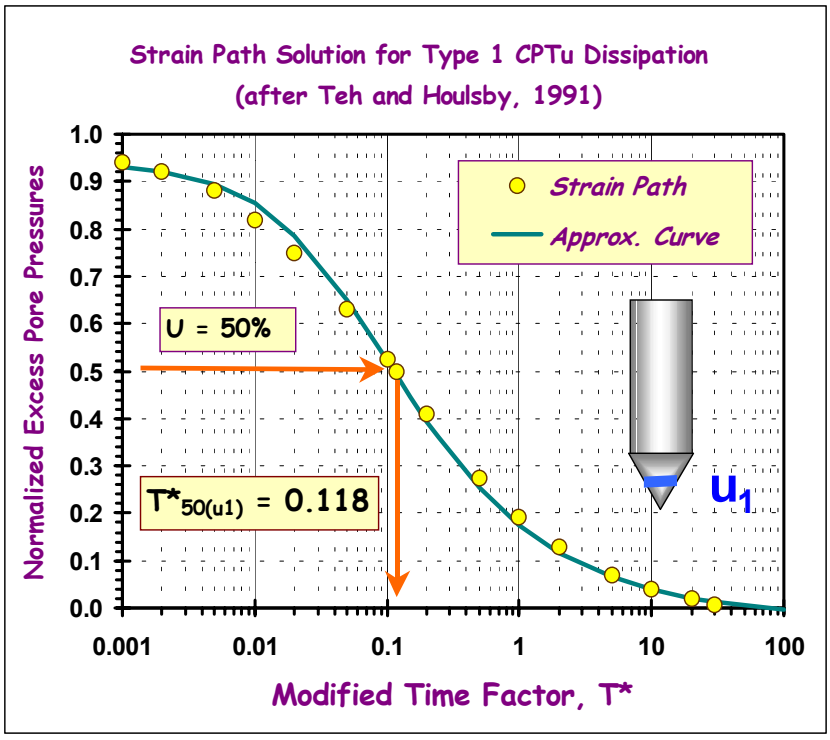

Figure 9-43a. Modified Time Factors for u_1 Monotonic Porewater Dissipations

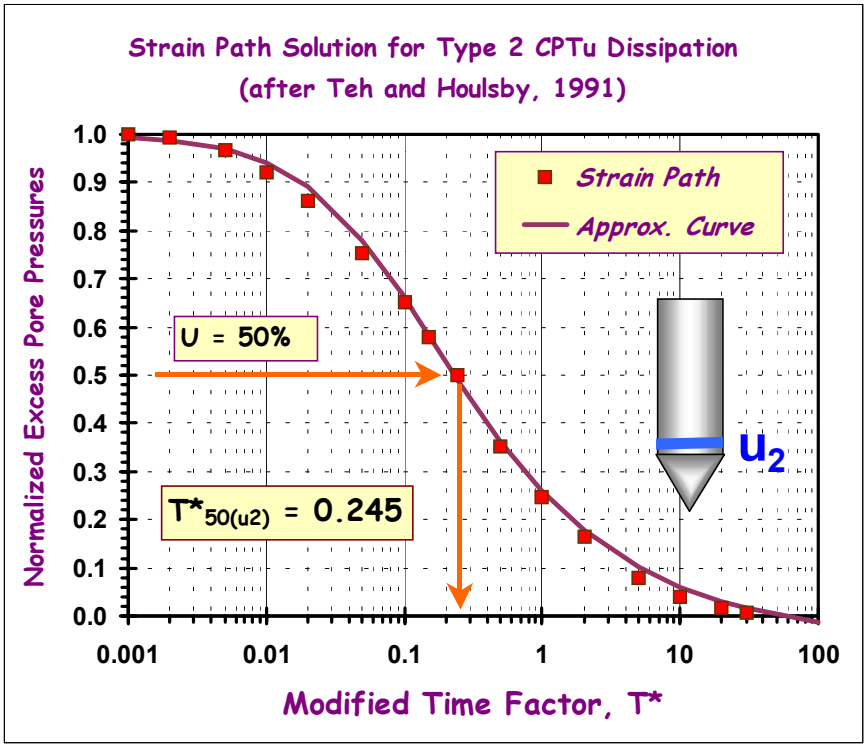

Figure 9-43b. Modified Time Factors for u_2 Monotonic Porewater Dissipations

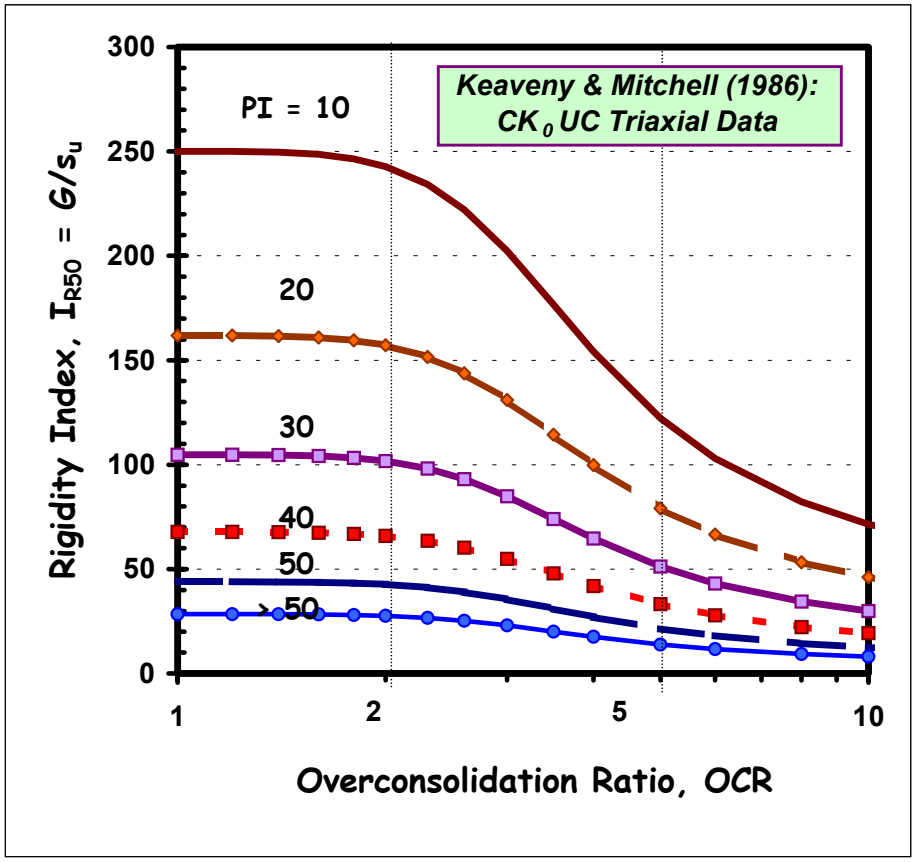

Figure 9-44. Estimation of Rigidity Index from OCR and Plasticity Index (Keaveny & Mitchell, 1986).

For clays, the rigidity index (I_R) is the ratio of shear modulus (G) to shear strength (s_u) and may be obtained from a number of different means including: (a) measured triaxial stress-strain curve, (b) measured pressuremeter tests, and (c) empirical correlation. One correlation based on anisotropically-consolidated triaxial compression test data expresses I_R in terms of OCR and plasticity index (PI), as shown in Figure 9-41. For spreadsheet use, the empirical trend may be approximated by:

$$I_R \approx \frac{\exp\left[\frac{137 - PI}{23}\right]}{\left[1 + \ln\left\{1 + \frac{(OCR - 1)^{3.2}}{26}\right\}\right]^{0.8}} \qquad (9\text{-}30)$$

Additional approaches to estimating the value of I_R are reviewed elsewhere (Mayne, 2001).

To facilitate the interpretation of c_h corresponding to t_{50} readings using the standard penetrometer, Figure 9-42 presents a graphical plot for various I_R values.

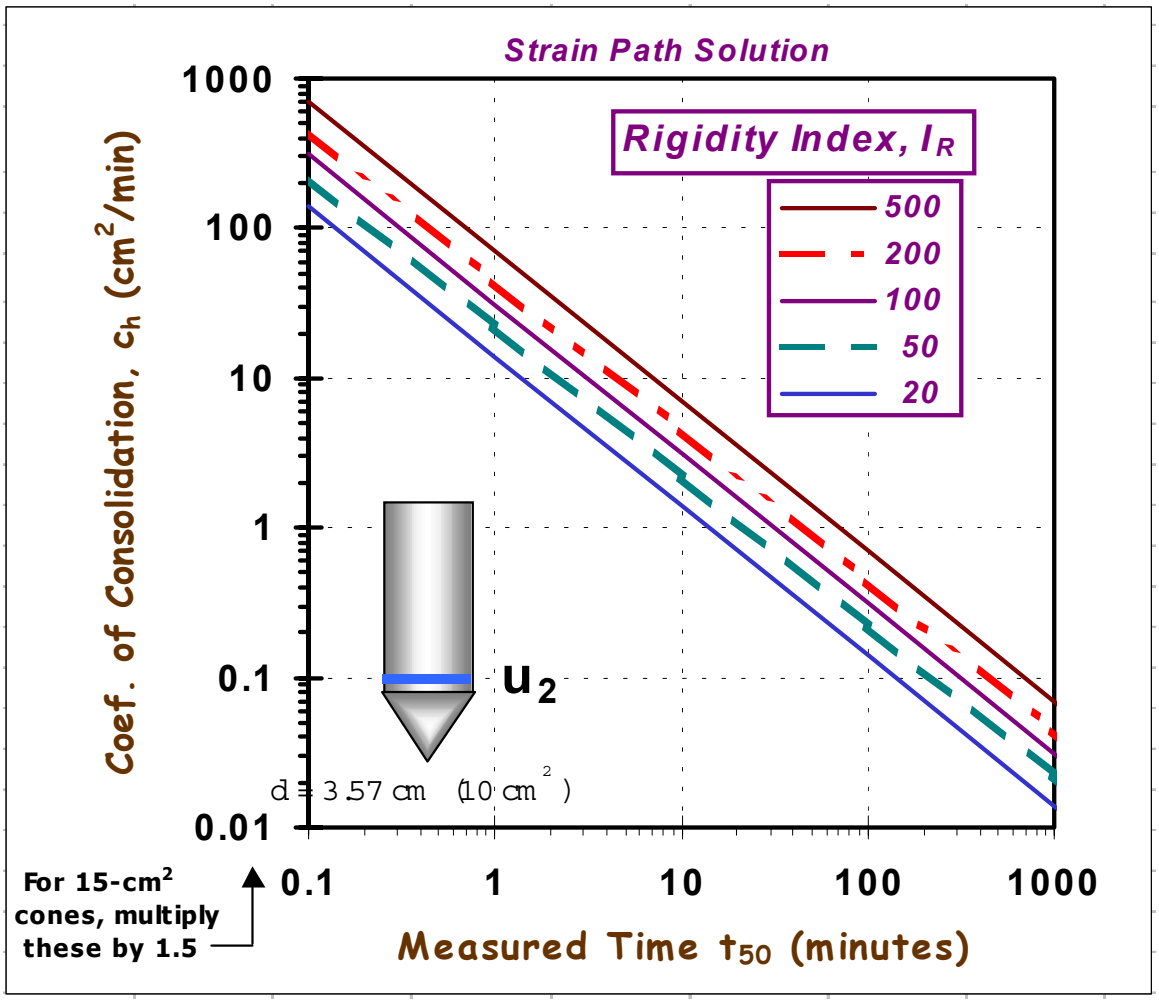

Figure 9-45. Coefficient of Consolidation for 50% Dissipation from Shoulder Readings

9.6.2. Dilatory Dissipations

In many overconsolidated and fissured materials, a dissipation test may first show an increase in Δu with time, reaching a peak value, and subsequent decrease in Δu with time (e.g., Lunne, et al. 1997). This type of response is termed *dilatory* dissipation, referring to both the delay in time and cause of the phenomenon (dilation). The dilatory response has been observed during type 2 piezocone tests as well as during installation of driven piles in fine-grained soils. The definition of 50% completion is not clear and thus the previous approach is not applicable.

A rigorous mathematics derivation has been presented elsewhere that provides a cavity expansion-critical state solution to both monotonic and dilatory porewater decay with time (Burns & Mayne, 1998). For practical use, an approximate closed-form expression is presented here. In lieu of merely matching one point on the dissipation curve (i.e, t_{50}), the entire curve is matched to provide the best overall value of c_h. The excess porewater pressures Δu_t at any time t can be compared with the initial values during penetration (Δu_i).

The measured initial excess porewater pressure ( ) $u_i = u_2 - u_o$) is given by:

$$) u_i = ( ) u_{oct})_i + ( ) u_{shear})_i \qquad (9\text{-}31)$$

where $( ) u_{oct})_i = F_{vo} r (2M/3)(OCR/2)^{7} \ln(I_R)$ = the octahedral component during penetration;

and $( ) u_{shear})_i = F_{vo} r [1 - (OCR/2)^{7}]$ is the shear-induced component during penetration.

The porewater pressures at **<u>any</u>** time (t) are obtained in terms of the modified time factor T* from:

$$) u_t = ( ) u_{oct})_i [1 + 50 Tr]^{-1} + ( ) u_{shear})_i [1 + 5000 Tr]^{-1} \qquad (9\text{-}32)$$

where a different modified time factor is defined by: $Tr = (c_h t)/(a^2 I_R^{0.75})$. On a spreadsheet, a column of assumed (logarithmic) values of Tr are used to generate the corresponding time (t) for a given rigidity index (I_R) and probe radius (a). Then, trial & error can be used to obtain the best fit c_h for the measured dissipation data. Series of dissipation curves can be developed for a given set of soil properties. One example set of curves is presented in Figure 9-43 for various OCRs and the following parameters: $7 = 0.8$, $I_R = 50$, and $Nr = 25^{\circ}$, in order to obtain the more conventional time factor, $T = = (c_h t)/a^2$.

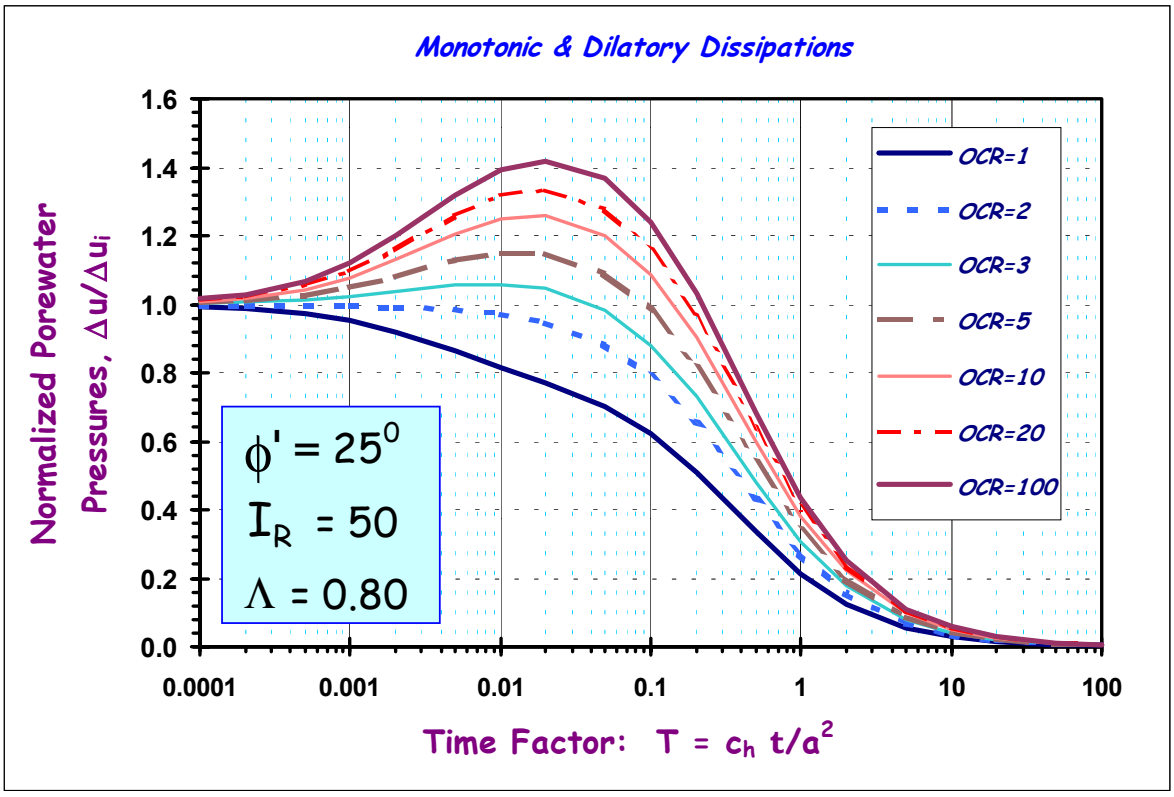

Figure 9-46 Representative Solutions for Type 2 Dilatory Dissipation Curves at Various OCRs (after Burns & Mayne, 1998).

9.7 NONTEXTBOOK MATERIALS

The aforementioned relationships have been developed for “common” geomaterials, including clays and silts of low to medium sensitivity and uncemented quartz sands. The geotechnical engineer should always be on the lookout for unusual soils and complex natural materials, as Mother Earth has bestowed a vast and varied assortment of soil particles under many different geologies and origins. In many parts of the world, notoriety is associated with highly organic soils such as peats, bogs, muskegs, and organic clays & silts. In some settings, sensitive soils and quick clays may be found. These soils should be approached with great caution and concern over there short- and long-term behavior with respect to strength, stiffness, and creep characteristics.

In certain locations, cemented sands of calcareous origin or corraline deposits (carbonate sands) are found and these exhibit significantly different behavior to loading than the more ubiquitous quartz sands. Other nontextbook soil types include diatomaceous earth, dispersive clays, collapsible soils, loess, volcanic ash, and special structured geomaterials. When in doubt, additional testing and outside consultants should be brought in to assist in the evaluation of the subsurface conditions and interpretation of soil properties. Although these may seem like extra expenses from an initial viewpoint, in the unfortunate scenario of a poorly-designed facility, the overall immense costs associated with the remediation, repair, failure, and/or ensuing litigation will far outweigh the small investigative costs up-front.

Finally, man-made geomaterials have emerged in the past century, bringing many new and interesting challenges to geotechnique. These include vast amounts of tailings derived from mining operations related to extraction of copper, gold, uranium, phosphates, smectities, and bauxite. These tailings disposals include earthen dams that empound slimes that are unconsolidated, thus requiring periodic checks on stability of slopes under static and dynamic loading. Other man-made geomaterials include modified ground from site improvement works such as vibroflotation, dynamic compaction, and grouting. Artificial "soils" include the very large deposits of waste (or "urban fill") and construction of immense landfills across the U.S. These, in particular, offer new demands for site characterization technologies because of the unusual and widely-diverse nature of these landfilled substances.